INVESTIGATION OF GAS PHASE FRAGMENTATION MECHANISM OF DOUBLY CHARGED *a* IONS BY MASS SPECTROMETRY

A Thesis Submitted to
the Graduate School of Engineering and Sciences of
İzmir Institute of Technology
in Partial Fulfillment of the Requirements for the Degree of

MASTER OF SCIENCE

in Biotechnology and Bioengineering

by
Doğacan KIZILKOCA

July 2019
İZMİR

We approve the thesis of **Doğacan KIZILKOCA**

Examining Committee Members:

Prof. Dr. Talat YALÇIN
Department of Chemistry, İzmir Institute of Technology

Prof. Dr. Nuran ELMACI IRMAK
Department of Chemistry, İzmir Institute of Technology

Assist. Prof. Dr. Ayşe Banu DEMİR
Department of Basic Medical Sciences, İzmir University of Economics

12 July 2019

Prof. Dr. Talat YALÇIN
Supervisor, Department of Chemistry
İzmir Institute of Technology

Doc. Dr. Alper ARSLANOĞLU
Co-Supervisor, Department of
Molecular Biology and Genetics
İzmir Institute of Technology

Assist. Prof. Dr. Engin ÖZÇİVİCİ
Head of the Department of Bioengineering

Prof. Dr. Aysun SOFUOĞLU
Dean of the Graduate School of
Engineering and Science

ACKNOWLEDGMENTS

Firstly, would like to thank my research advisor Prof. Dr. Talat YALÇIN for my both undergraduate and graduate years. He always believed and supported me at every difficulty, and it was an honour of me studying Biological Mass Spectrometry Laboratory leadership of him. Besides to all scientific points, his fatherly behaviours will not be forgotten. I am also grateful to rest of my thesis committee Prof. Dr. Nuran ELMACI IRMAK and Assist. Prof. Dr. Ayşe Banu DEMİR.

I would like to express my gratitude to Naturin Nutraceuticals and Akdeniz Kimya family for giving me the opportunity to work and complete my master degree at the same time.

Furthermore, I am deeply grateful to my dear friends Seren ŞEN, Anıl Can Aydın, Hakan KAYA, Bora BEKMEZCİ, Okan ERDOĞAN, Cihan ALP, İsmet Arınç AYTAÇ, Erdi GÜLŞEN and Begüm ÖZYAĞCI for supporting me at all challenging times. This is very important for me, thank you guys!

Special and crucial thanks to Furkan AKSOY and Aslı Gülce BARTAN for being more than a friend to me. They support me at both good and bad days of mine. It could be very difficult and unendurable without your help. I will always miss our sweet home! I dearest thanks to my fiancé and my future wife Damla AKSOY for her endless love, understanding, tolerance, and patience. She has been with me for nine years to make every moment perfect. Feeling that I was with her when I lost all my strength and hope made me come today. She makes my life meaningful by loving me. Thank you.

Last but not least, I owe my endless thanks to my father Hakan KIZILKOCA, my sister Şelale KIZILKOCA and my lovely mother Fisun KIZILKOCA who is always beside to me with her great motivation and believes in me more than everybody. I really appreciate for being always patient with me. Finally, thank you so much for raising me as a kind and loving person, I will always proud to be a part of our family.

ABSTRACT

INVESTIGATION OF GAS PHASE FRAGMENTATION MECHANISM OF DOUBLY CHARGED *a* IONS BY MASS SPECTROMETRY

This dissertation presents studies of gas-phase fragmentation mechanism of doubly-charged a_7 ions from basic amino acid containing model peptides under low-energy collision-induced dissociation (CID). The study includes three sets of C-terminal amidated model peptides which are alanine series containing basic amino acids (His – Arg – Lys). Position of His, Arg and Lys residue is varied from N-to-C terminal. Both positional effect and peptide sequence effect were examined for the fragmentation reactions of doubly-protonated a_7 ions for these heptapeptides.

The CID-MS^4 mass spectra of doubly-protonated a_7 ions have internal amino acid losses which provide a piece of evidence for macrocyclization reaction. The proposed reaction mechanism involves the production of doubly-charge *a* ions and charge-separation reaction of doubly-protonated *a* ions in the gas-phase which generates a protonated direct and non-direct *a* ion. All model peptides were also studied to understand the behaviour of doubly-protonated *a* ions better. Direct and non-direct sequence fragmentations which are singly or doubly protonated were observed for all studies. The reactions mechanisms were adjusted according to the results.

In conclusions, the results presented in this dissertation can be used to elucidate the correct and reliable peptide sequences, and this improve protein identification strategies which are required for high-throughput proteomic studies.

ÖZET

ÇİFTE PROTONLANMIŞ *a* İYONLARININ GAZ FAZI PARÇALANMA MEKANİZMALARININ KÜTLE SPEKTROMETRE İLE İNCELENMESİ

Bu tez, çarpışma ile indüklenmiş ayrışma (CID) altında, bazik amino asit içeren model peptitlerden elde edilen çift-protonlanmış *a* iyonlarının gaz fazı parçalanma mekanizmalarının araştırılmasını içermektedir. Çalışmada, bazik amino asitlerin konumlarının, peptidin N-ucundan C-ucuna doğru değiştiği üç farklı model alanin peptit dizi kullanılmıştır. Bazik amino asitlerin konumlarının ve peptit dizilimlerinin, çift-protonlanmış *a* iyonlarının parçalanma reaksiyonları üzerindeki etkişi araştırılmıştır.

Çift protonlanmış *a* iyonlarının çarpışma ile indüklenmiş ayrışma etkisi altında çok aşamalı kütle spektrometrisi (MS^4) spektrumlarında macrohalkalaşma tepkimesine kanıt olacak kopmalar gözlenmiştir. Önerilen reaksiyon mekanizmaları gaz fazındaki çifte-protonlanmış *a* iyonlarının yük-ayrımı reaksiyonu oluşturulması ve ardından peptitden içsel ve içsel olmayan *a* ve *b* iyonları oluşturmasına dayanmaktadır. Ayrıca yapılan tüm çalışmalar çifte protonlanmış *a* iyonlarının gaz fazındaki davranışlarını daha iyi anlama amacını taşımaktadır.

Sonuç olarak, bu çalışmalarda gösterilen sonuçlar peptit sekanslarının doğru ve güvenilir bir şekilde açıklamak için kullanılabilinir ve bu durum proteomik çalışmalar için gerekli olan protein tanımlama stratejilerini geliştirebilir.

Dedicated to;

the memory of my lovely grandmother Nurten KIZILKOCA

and

the memory of my grandfather Abdül ÖZPEHLİVAN

TABLE OF CONTENTS

LIST OF FIGURES

Figure **Page**

Figure **Page**

LIST OF TABLES

Table **Page**

CHAPTER 1

MASS SPECTROMETRY

1.1. What is Mass Spectrometer?

Mass spectrometry (MS) is a powerful analytical technique which produces gas-phase ions from different kind of samples and used to separate those ions based on their mass-to-charge ratio *(m/z).* This method can be practical to the extensive range of area such as forensic, organic synthesis, drug testing, chemistry, archaeology, geology and petroleum industry.

In the late 1800s Sir Joseph John Thomson's studies about the conduction of electricity through gases was beginning of a discovery of electrons. Therefore, The Nobel Prize in Physics 1906 was awarded to Joseph John Thomson "*in recognition of the great merits of his theoretical and experimental investigations on the conduction of electricity by gases.*" Thomson studied positively charged ions in 1906 but, this work was only a beginning for another famous discovery in 1912. After that, Thomson and his research group studied about stable isotopes of neon on a photographic plate concerning for their path in the magnetic and electric field. This study led Sir J.J. Thomson to be called the father of mass spectrometry.

Ionization techniques that discovered and developed previously were not convenient for studying biological molecules of large molecular mass such as proteins, lipids and oligonucleotides etc. For this reason, electrospray ionization (ESI) and Matrix-assisted laser desorption ionization (MALDI) which are soft ionization techniques have been developed. In this way, non-volatile and thermally unstable large compounds are passed into the gas phase without degradation.

Mass spectrometers consist of three major components: an ionization source, a mass analyzer, and an ion-detector. (Figure 1) The first main step is generating charged particles (positively or negatively charged) by the ionization source after introducing analyte. Because almost every ionization technique working principle needs gas phase molecules, the analyte must transfer to the ionization source as a gas phase molecule.

Then, the ions are directed to the analyzer by the electric field and they are separated according to their m/z values. After that, the ions from the analyzer are interpreted as an electrical signal by the detector and transferred to the computer. Lastly, these signals are monitored as a mass spectrum which is a bar graph of relative abundance of the ion (ion intensity) versus the m/z ratio.

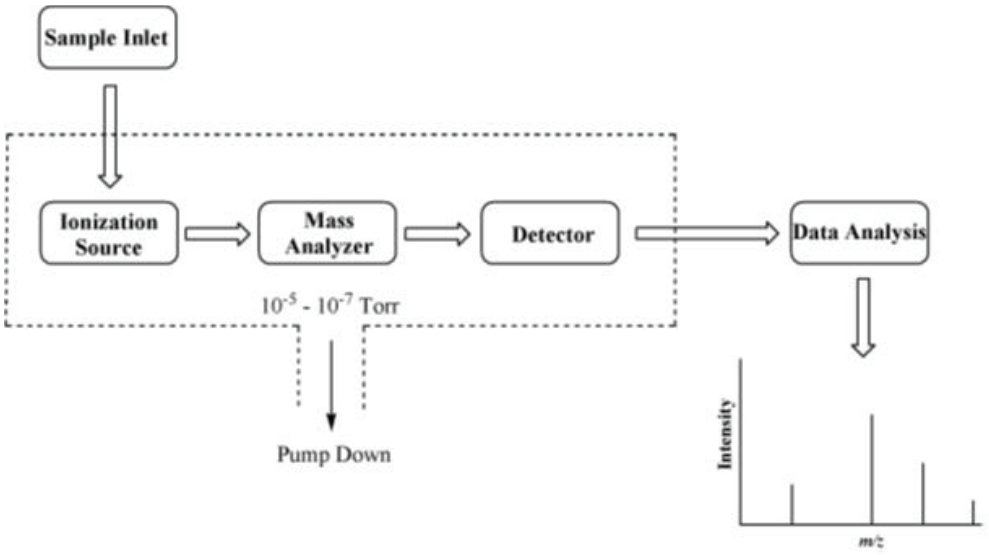

Figure 1. Basic components of a mass spectrometer (Source: Banerjee, et al. 2012)

As shown in Figure 1 above the ionization source, mass analyzer and detector are performed under high vacuum (low pressure). Ions which are generated in the source must be able to reach to the detector. Therefore, vacuum systems avoid any chance of collision or interaction between ions or other molecules. Generally high vacuum conditions are optimized to 10^{-5} or 10^{-7} Torr by two pumping stages. First one is a mechanical pump and the second one is a turbomolecular pump.

1.2. Ionization Techniques

To perform the analysis in the mass spectrometer, the sample must first be charged and ionized after analyte be introduced to the device. From past to present there are many types of ionization techniques which are electron ionization (EI), chemical ionization (CI), secondary ion mass spectrometry (SIMS), laser desorption ionization (LDI), field ionization (FI), plasma desorption (PD), fast atom bombardment (FAB), thermospray ionization (TS), electrospray ionization (ESI), matrix-assisted laser desorption/ionization (MALDI), and most recently direct analysis in real-time (DART). They are basically named ‘soft’ or ‘hard’ techniques. When considering the hard ionization techniques, they

are highly energetic, and this condition causes the generation of many fragmentation ions. Although, EI was the first hard ionization source, limited to volatile, thermally stable and small molecular weight.

Inability to perform biological molecules (proteins, peptides, etc.) because of the limitations has led to the discovery of a soft ionization technique. In this process, less or no fragmentation is observed. The most commonly used soft techniques are EI and MALDI.[1]

1.2.1. Electrospray Ionization (ESI)

Although the electrospray process has been known for a long time, the main process of thinking about ESI-MS was initiated by Prof. Dole in 1960s, who was a physical chemist at Northwestern University. Then in the 1980s, John B. Fenn and his research group introduced ionization of large biomolecules by combination ESI with MS, thus a new era for proteomic studies has begun.[2]

ESI process can be explained with three major steps. First one is the formation of charged (ionized) droplets, the second one is the fission of those droplets and then finally the formation of desolvated ions. More detailly, analyte and organic solvent solution introduced from the injection part which includes a mechanical syringe or chromatographic system with a continuous flow to stainless steel capillary needle. When the analyte injected, a very high positive or negative voltage is applied (±2-6 kV) and cause the formation of charged droplets. The applied electric field separates the positive and negative ions in the analyte solution and allows the desired ions to move. Then, desired ions (depends on working on positive or negative mode) accumulate as droplets which form a Taylor cone. As soon as the spraying process takes place, the samples are exposed to nitrogen gas (N_2). In this case, solvent evaporation takes place because of the collide with the inert N_2 gas as a nebulizing gas. As the evaporation continues, the droplets gradually shrink. This causes an increase in the charge density at the droplet surface. As a result, coulombic repulsion between the charges becomes greater than the surface tension, causing the balance between the surface tension and the electrostatic attraction is broken (Rayleigh instability limit) thus, the coulombic explosion occurs. Finally, charged particles were generated and directed to the analyzer (Figure 2).[3-4]

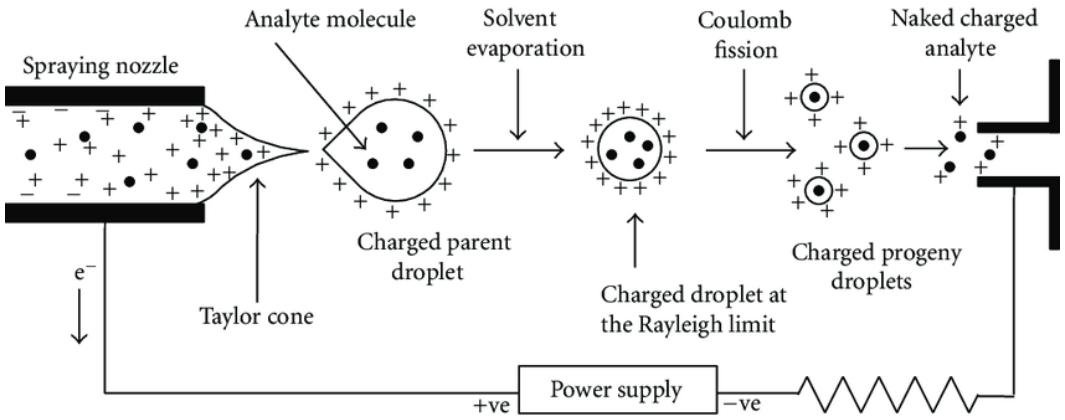

Figure 2. Schematic representation of the ESI ion source

(Source: Banerjee, et al. 2012)

To ability to generate multiply charged ions of large biomolecules is crucial. This feature allows large molecules to be observed in the instrument in the small mass range. In other words, ESI can ionize proteins which have very large molecular weight Another advantage is that the ESI can be used in combination with liquid chromatography (LC) and different analyzers such as quadrupole, ion trap and time-of-flight mass can be used with ESI.

1.2.2. Matrix-Assisted Laser Desorption/Ionization (MALDI)

Matrix-assisted laser desorption/ionization, namely MALDI, is a very important, powerful and widely used solid-phase ionization technique because it can ionize non-volatile and thermally labile macromolecules which have large molecular weight such as peptides, proteins, other biomolecules, and polymers. MALDI was first introduced by Koichi Tanaka (1988) and Michael Karas & Franz Hillenkamp (1988) at almost the same time.[5] MALDI is generally obtained in two steps. First one is dissolving analyte in a suitable volatile solvent, called the matrix. Molecules in the solvent, must have a very strong ultraviolet (UV) absorption and typical matrix solution concentration ratio is 1:1000 (analyte/matrix). Weak organic acids which have an aromatic ring can be used as a matrix. Because of the electron delocalization on the aromatic ring, the matrix has chromophore property and ability to absorb laser energy. According to that, it behaves as a proton donor or accepter during desorption. The solution mixture is placed into a multi-position sample target plate and the mixture containing the analyte allows to completely dry and co-crystalize by removing the liquid solvent used in preparation before analysis.

The second step involves irradiation of solid solution by pulsed UV-laser under vacuum conditions in the source part. Nitrogen laser at 337 nm and neodymium-doped yttrium aluminium garnet (Nd: YAG) at 335 nm are widely used lasers.[6]

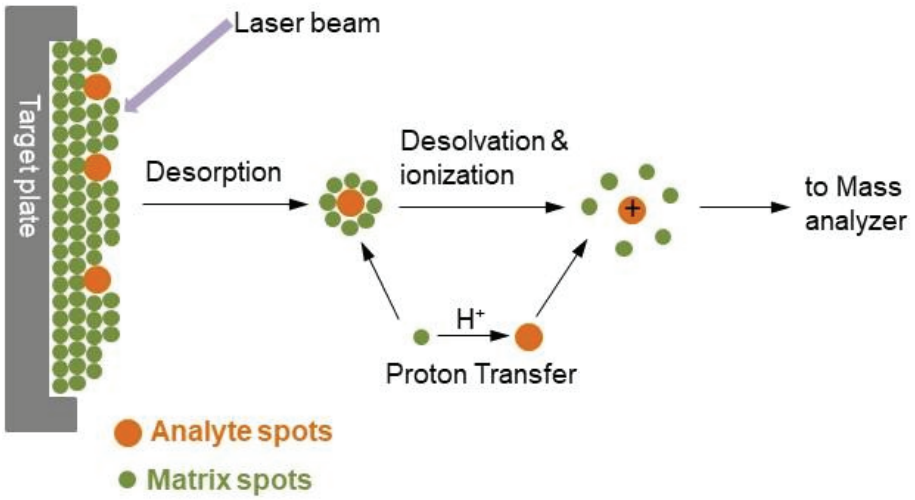

Figure 3. Ionization of analytes by MALDI (Source: Lane 2005)

The laser beam is applied on the solid mixture and the matrix absorbed the energy which is from the laser pulse thus, the matrix begins to heat up. This energy also transferred to the analyte as heat. Then, matrix and any analyte embedded in the matrix are vaporized together from the solid-state into the gas-phase ions. Finally, this technique generates gas-phase ions without fragmentation and directed to the mass analyzer by an electric field. MALDI generally generates mainly singly or doubly charged ions.

Despite the mechanisms of desorption and ionization in MALDI are still not well-known, there are some suggested pathways by Zenobi and Knochenmuss in1998 and Dreisewerd in 2003. They are gas-phase photoionization, excited-state proton transfer, ion-molecule reactions and desorption of performed ions.[6-7]

Compared to other laser ionization techniques, MALDI is more successful and sensitive thanks to the matrix. The matrix absorbs most of the energy which is from laser pulse so, it minimizes the sample damage and increases the efficiency of energy transfer. Also, the matrix prevents the aggregation of analytes by separating the analyte molecules from one another. Sample preparation and Matrix-analyte composition are the most important part to get high shot-to-shot reproducibility and high-quality ion signals in MALDI-MS. The decision of which matrix to use depends on the type of analyte. Most commonly used ones are nicotinic acid (266 nm) for proteins and peptides, 2,5-dihydroxybenzoic acid (337-353 nm) for proteins, peptides and some polymers, sinapinic

acid (337-353 nm) for proteins and peptides, α-cyano-4-hydroxycinnamic acid (337-353 nm) for peptides, 3-hydroxy-picolinic acid (337-353 nm) for nucleic acids[8-9]. Their structures showed in Figure 4 .

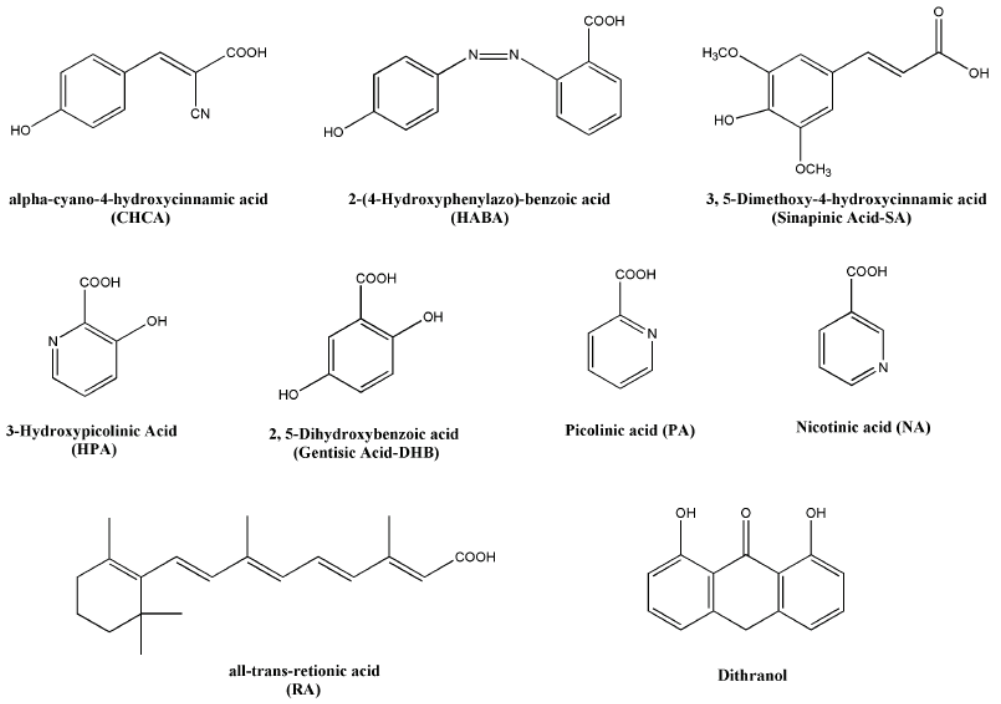

Figure 4. Preferred matrices in MALDI-MS (Source: Laugesen and Roepstorff 2003)

Liquid chromatography system can be used both in MALDI and ESI. Except that, the spotter must be used in MALDI because sample and matrix must be mixed before the analysis. Tolerance to salt and certain buffer concentration is one of the big advantages of MALDI compared to the ESI.[10]

1.3. Mass Analyzer

As mentioned, after the generation of gas-phase ions in sources, they are directed to the mass analyzer. Then, analyzers separate ions according to their *m/z* ratio rather than their mass alone. With the invention of various ion sources and their usage, different type of mass analyzers needed. Electric and magnetic fields are driving forces of analyzers. They can be used single or combined. This situation also creates the basic differences among all analyzers. Nowadays, the most commonly used analyzers are time-of-flight (TOF), quadrupole (Q), ion-trap (IT), Fourier transform ion cyclotron resonance (FT-ICR), and Orbitrap. When TOF, Q and IT are known as electric analyzers, FT-ICR principle has a magnetic field. All analyzers have advantages and disadvantages

depending on the what is desired but, have the same characteristics for performance such as mass accuracy, mass range, resolution, transmission, speed and, ability to perform tandem MS.

1.3.1. Quadrupole (Q)

In the 1950s, Nobel Prize-winning physicist Paul Wolfgang described quadrupole analyzer for the first time and it was started to be widely used in a short time because of fast scan rate, high transmission efficiency and, compact size. Quadrupoles consists of four parallel electrical rods assembled in two pairs in the *x-y* plane as shown in Figure 5. They transmit an ion which has specific *m/z* ratio to the detector and because of that they are also called mass filters.[11-12] When radio frequency (RF) is applied one of the two opposite rods, direct current (DC) is applied to the other ones. Therefore, rod pairs positively and negatively charged, and they are connected by electricity. DC and RF voltages create an oscillating electric field which behaves like a filter to transmit selected *m/z.* After producing the ions in the source chamber, they are introduced to the quadrupole continuously. While the specific RF and DC voltages are applied the rods, only some ions which have a specific *m/z* ratio can pass through the analyzer in the z direction and reach detector. This situation explains is that, single m/z ions preserve their trajectories from source to the detector, whereas ions with different m/z ratio (greater or lesser) cannot maintain stable trajectories and analysis journey of that ion is failed.[13-14]

Low cost, robustness, compact size etc. are advantages of the quadrupole. However, it has some limitations such as mass range (< 4,000 Da), low resolution and not being able to do MS/MS studies. Addition of an extra quadrupole can be a solution of MS/MS limitation (triple quadrupole) with the use of the second one as a collision cell and the others as a scanner (responsible for scanning).

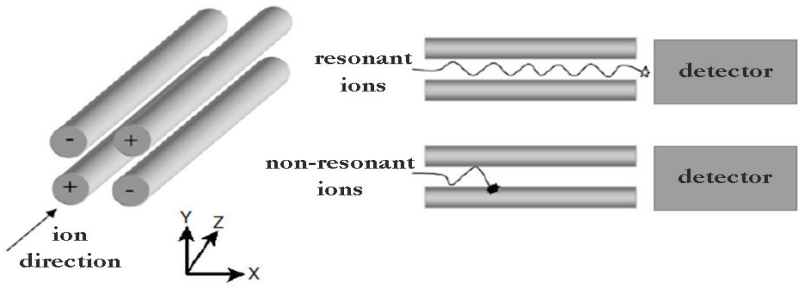

Figure 5. A quadrupole mass analyzer (Source: Liebler 2002)

1.3.2. Ion Trap (IT)

Although the idea of ion trap was first introduced in 1950, its widespread use in mass spectrometry was in 1984. Paul and Steinwedel announced ion-trap in the 1950s, and Stafford and his co-workers developed the idea in 1984 to make them more qualified. Later, Wolfgang Paul and Hans Dehmelt were awarded the Nobel Prize in Physics in 1989.[15]

Ion trap has 2 different variations, 2D and 3D. The 3D ion trap is also called the quadrupole ion trap (QIT). In this device, ions are exposed to a rf field, but forces occur in all three dimensions instead of two dimensions. The stable motion of the ions in the linear quadrupole gives rise to a free movement area in the z direction and that motion does not allow degrees of freedom. Therefore, ions are trapped from three electrodes-a ring electrode and two end-cap electrodes of hyperbolic cross-section, which are the parts that make up the QIT (Figure 6).

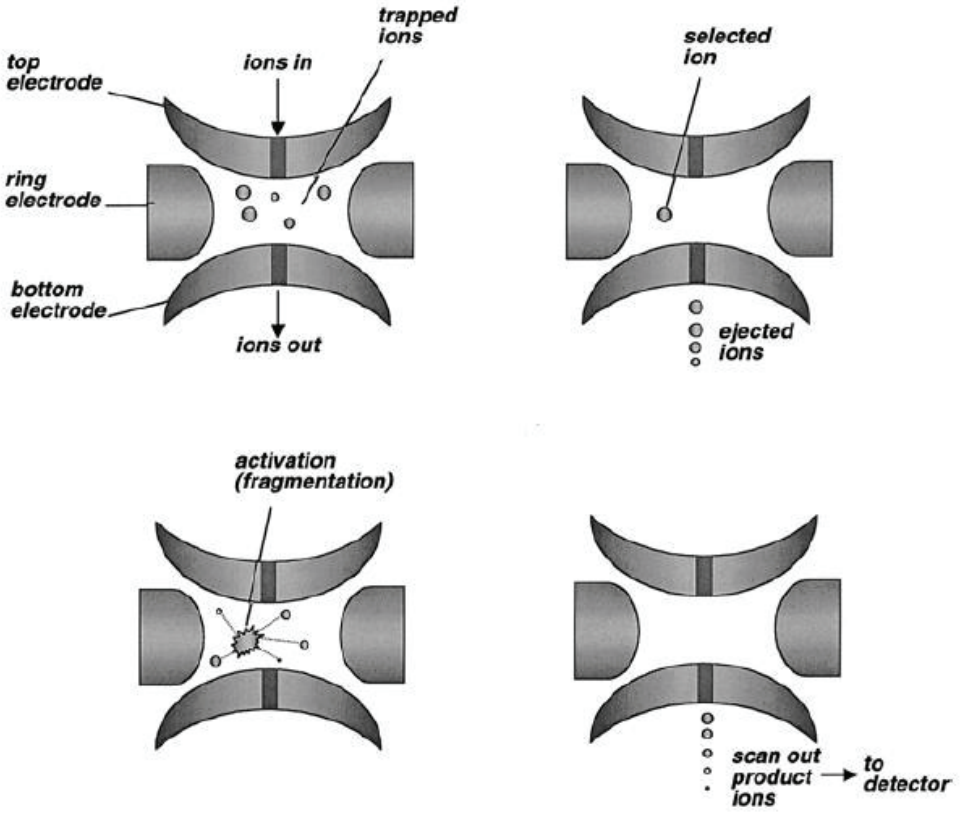

Figure 6. Schematic Diagram of an Ion-Trap (Source: Liebler 2002)

Unlike the quadrupole which uses DC voltage, the ring electrode exposes ions to the RF voltage to generate an oscillating electric field and that field of force starts to oscillate ions in eight-shaped trajectory related to their *m/z* ratio. The trapped ions cause deterioration of the electric field due to coulombic interactions. To avoid the collision, helium (He) gas is introduced to the system. It is also called bath gas or target gas. In addition to reducing the kinetic energy of the ions, this gas allows the ions to be held in the middle of the trap to increase the mass resolution and sensitivity. When RF and DC potentials are increased, ions become more unstabilized for higher *m/z*. As a result of this, they are expelled from the trap. Oscillating frequencies of an ion is a characteristic feature for ion masses. Therefore, the voltage and time required by the ions to leave the trap will differ depending on the *m/z* of the ions.[16]

The most important advantages of QIT are high sensitivity, mechanical convenience and compactness, availability for MS^n experiments (tandem mass spectrometry analysis), and high resolution.

1.3.3. Time-of-Flight (TOF)

Other types of mass analyzers are time-of-flight analyzers which were described by Stephens in 1946. Design of a linear TOF (LTOF) mass spectrometer was published in 1955 by Wiley and McLaren and this instrument was the first commercial one. The main principle of TOF is measuring the time of the ion's movement from analyzers entrance to the end. In other words, it measures the mass dependent time it takes ions which have different masses in the field-free drift tube. Explanation of the field-free is that, there is no electric field or magnetic field applied to the ions during their flight in the tube. As is understood, there is a need to know the exact time when the ions are formed in the ion source and leave the source. Therefore, MALDI, a laser-pulsed ionization technique is very suitable for TOF mass analyzers. After MALDI produces the ions, accelerations of ions to a field-free region with the same kinetic energy is occurred because of the potential difference between electrodes and entry grid. When the ions gain kinetic energy, their velocity will start to differ because they have different masses. Therefore, ions start to fly with different velocities to reach the detector in the field-free region. The relationship between ions velocities and their *m/z* ratios is inversely proportional. That fact explains that, movement (flight) of the lighter ions is faster than the heavier ones in the flight tube so, ions which have small *m/z* ratio reach the detector

earlier. All the ions which are produced from MALDI or anther pulse source reach the detector one by one and separations occur based upon their velocity differences. Hence, measuring the time of ions movement in field free region from the source to the detector is used to determine the *m/z* ratios. A linear TOF tube is illustrated in Figure 7.[17-18]

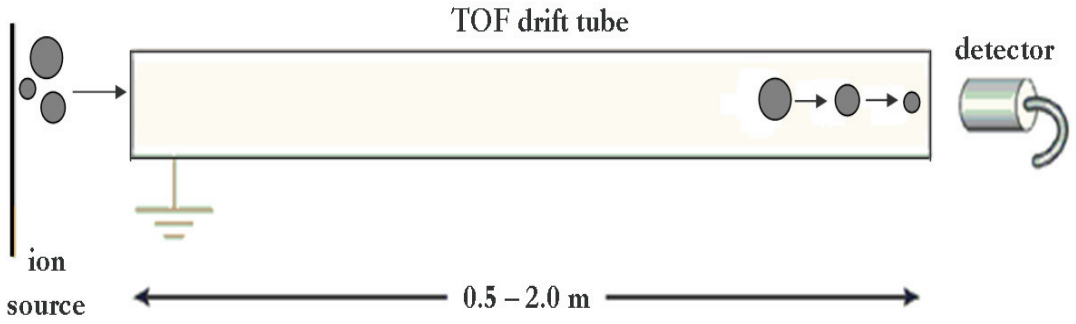

Figure 7. Schematic view of linear TOF mass analyzer

(Source: Glish and Vachet 2003)

After requirement simplifications are applied to the formula, m/z ratio is equal to $2eUt^2/L^2$. When the formulation is considered, it is seen that it depends on an elementary charge (e), an applied voltage (U), a length of drift tube (L) and a flight time (t), but not depend on the mass. This equation shows that, there is no upper mass range limit for TOF instrument. High transmission efficiency, high sensitivity, and very fast analysis speed are other advantages of TOF.

Kinetic energy distribution of ions having the same *m/z* ratio creates some issues and leads to poor mass resolution. To solve this problem, two types of solutions are introduced. First one is a short time lag or lag between ion formation and extraction. When the ions are formed in the source, they are expanded into a field-free region in the source. After a delay extraction of the ions to the outside is occurred. This technique is also known as pulsed ion extraction. (Figure 8)

The second solution is to use reflectron (Figure 9). It is an optical device which is located at the end of the drift tube and act as an electrostatic ion mirror. When the ions reach the end of drift tube, they are deflected by reflectron and it focuses them to the reflectron (second) detector. To correct of kinetic energy dispersion for ions having the same m/z ratio, higher kinetic energy which means faster ions spend more time in the reflectron and reach the detector at the same time than slower ones with the same *m/z*. Other words, reflectron provides longer flight time so, travel of ions in the field-free

region is more than liner mode. Therefore, using a combination of delayed extraction and reflectron improves the resolution.

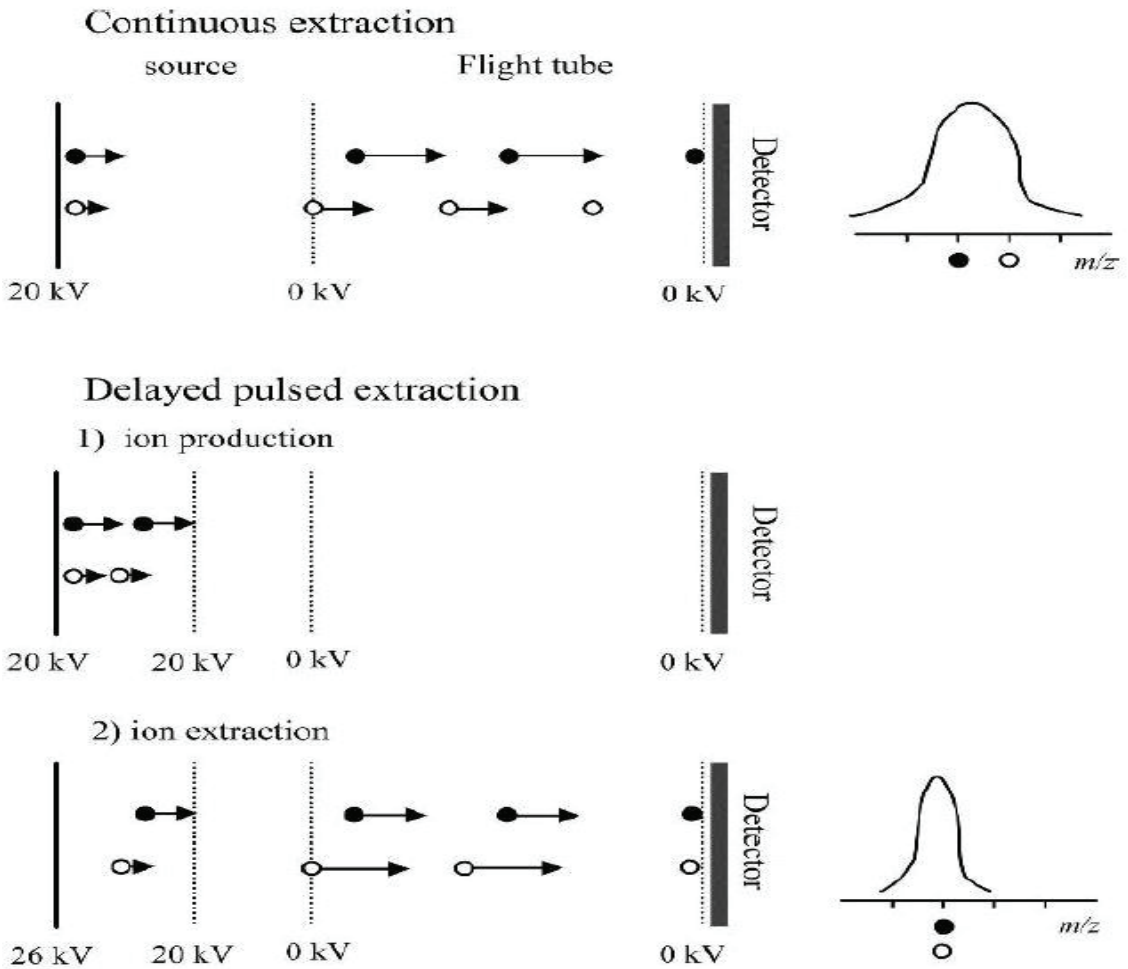

Figure 8. Schematic view of linear TOF mass analyzer

(Source: Glish and Vachet 2003)

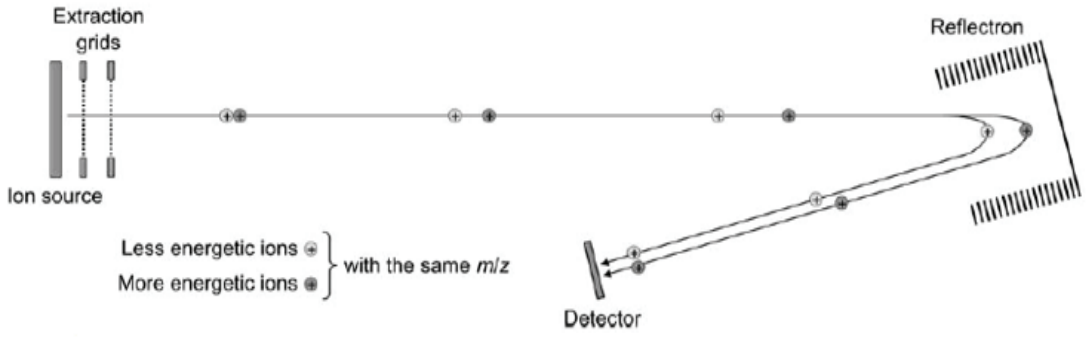

Figure 9. Basic components of a reflectron TOF analyzer (Source: Lane 2005)

Another technique which is called post-source decay (PSD) can be combined with reflectron TOF systems. The fragmentation of precursor ion takes place in the field-free region. Although precursor ion and fragment ion have different kinetic energies, they have the same velocity and same flight time absence of reflectron (LTOF). Having the same velocity for fragment ion and precursor ion means that, fragment ion has lower kinetic energy because of its lower mass. During ionization and acceleration to the flight tube, voltage is regulated to detect fragment ions.[17-18]

1.3.4. Fourier Transform-Ion Cyclotron Resonance (FT-ICR)

Another trapped-ion mass analyzer is ion cyclotron resonance (ICR) mass spectrometers and they are also called 'static' traps. Working principle of ICR is based on three main steps which are ionization, mass analysis and lastly detection. Magnetic field (B) is applied in the cubic cell (ion trap) and trapped ions start to move in cyclotron motion because of the magnetic field which is characteristic for every m/z ratio. When the ions are produced by an ion source (could be MALDI or ESI) they are sent to ion trap where has a magnetic field in it. Because of that ions move cyclotron motion which perpendicular to the magnetic field (Figure 10). The cubic cell made by three parallel plates. They are transmitter, receiver and, trapping plates. When the potential applied to the trapping plates, RF is applied to transmitter plates to increase the kinetic energy of the ions which means excitation of molecules. Detection is occurred as a time domain signal and then transforms to the *m/z* ratio with using Fourier transform (FT). Advantages of the FT-ICR are high mass resolution, easily MS/MS experiments, stable mass calibration and, high mass accuracy. Because of these features it is also the substantial device for proteomics analysis.[17, 19]

1.3.5. Orbitrap

Another analyzer using Fourier transform is Orbitrap analyzer. Makarov invented in 1996. An inner spindle electrode and two hollow outer concave electrodes are the major parts of orbitrap, illustrated in Figure 11. When one of the outer electrodes is open, ions get into it and this ion loading is tangential to the inner spindle electrode. Orbitrap analyzers create a potential between the inner spindle electrode and hollow outer concave electrodes. Unlike FT-ICR, they use an electric field (DC) to produce oscillations. Because of the potential, ions start to continuously spin around the inner spindle electrode

and oscillation observe back and forth. Finally, oscillation is measured and with the help of Fourier transform convert to mass spectra.

While the resolution is inversely proportional to the *m/z* in FT-ICR, it is inversely proportional to $(m/z)^{1/2}$ in orbitrap. Resolution and dynamic range are also increased compared to the Q-TOF.[17, 20]

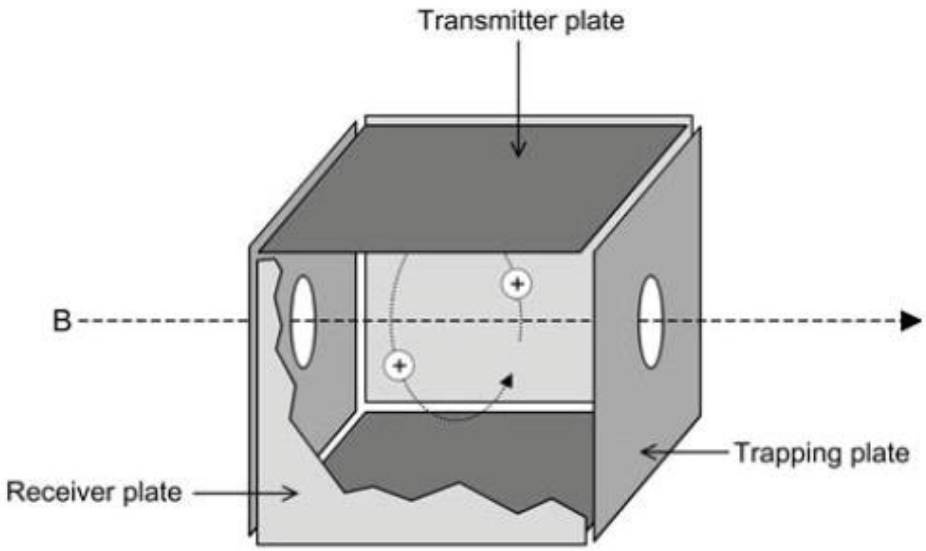

Figure 10. Schematic diagram of FTMS analyzer (Source: Lane 2005)

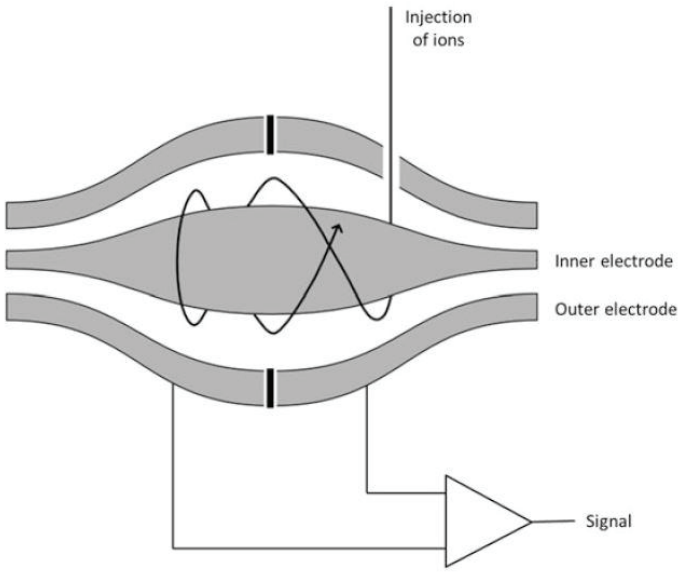

Figure 11. The electrostatic trap or orbitrap (Source: Hoffman, et al. 2007)

1.4. Detectors

Firstly, the ion beam which is generated in the ion source passes through an analyzer and separation are occurred based on their m/z ratio. Then, they are reaching to the detector where detection happens electrically. Finally, electrical detection which is the strike of the ions according to their m/z ratio transforms into a meaningful signal by the detector. Although, there are detectors with many different designs in market, expectations which are a large dynamic range, high stability, low noise, fast response time, high amplification, mass-independent response and, low cost are the same for all of them. The most familiar ones are a Faraday cup, an electron multiplier (EM), and a microchannel plate (MCP) in the market, but also photographic plates, scintillation counter detector, channel electron multipliers, resistive anode encoder image detectors, helium leak detectors, cryogenic detectors can be used for a different and specific analysis.[21]

1.4.1. Faraday Cup

Faraday cup is composed of a metal cup with a conducting electrode. That metal sheet can be made of GaP, CsSb, or BeO and also known as a dynode. When ions strike the dynode, it emits electrons and induce current. Then the current is amplified and recorded. (Figure 12)

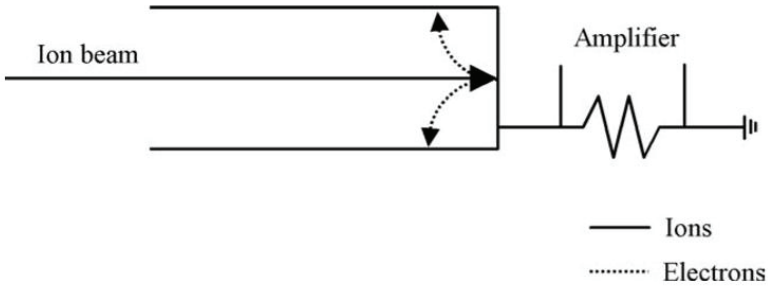

Figure 12. Schematic diagram of a Faraday cup (Source: Hoffman, et al. 2007)

1.4.2. Electron Multiplier

Electron multiplier (EMP) is a detector which consists of dynode series (Figure 13). An ion hits a surface of dynode and this causes the secondary ions emission which is released from the surface of dynode. These secondary ions can be positive, negative or neutral. Depending on the ions which are negative or positive, secondary particles

interests are also change. Although, the first dynode has a high voltage (-5kV), at the end of the multiplier voltage is almost ground potential. Because of that, when the ions strike the first dynode and causing the secondary electrons, acceleration has occurred for these electrons, so more electrons are formed. These strikes and multiplications will continue until the end of the multiplier and detection takes place. When the final electronic amplification is considered at the end, it is more than a million times.

1.4.3. Microchannel Plate

Microchannel Plate (MCP) is another type of detectors which is like electron multiplier but, it has many independent channels instead of a chain of dependent dynodes as shown in Figure 14. MCP is made of semiconductor channels and this feature is a directly related generation of secondary electrons when the ions hit the surface. Emission and detection of electrons increases gradually each time after the collision of secondary electrons to surface has occurred.[22]

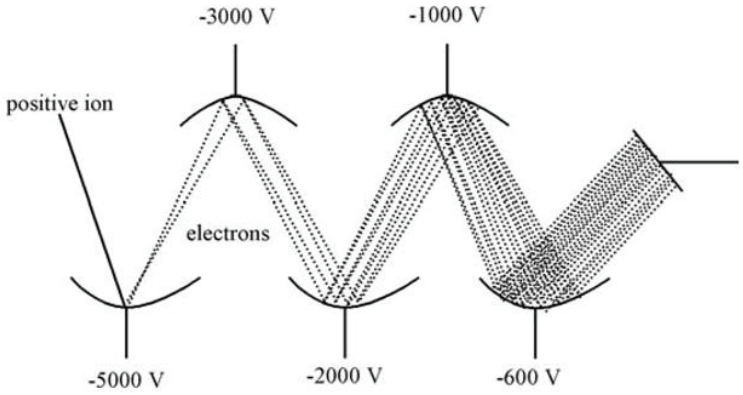

Figure 13. Schematic view of electron multiplier

(Source: Hoffmann and Stroobant 2007)

Figure 14. Schematic views of microchannel plate (Source: Hoffman, et al. 2007)

CHAPTER 2

FRAGMENTATION REACTION MECHANISMS OF PROTONATED PEPTIDES IN THE GAS-PHASE

Especially the invention of the soft ionization techniques such as ESI and MALDI, MS has become very popular for all researchers. As previously mentioned, soft ionization techniques have been used to analyze high mass bio molecules without any problem. Also, tandem mass spectrometry experiments (MS/MS) are allowed to obtain structural information of proteins or other biomolecules with high accuracy. Because of these developments, this thesis focusses on gas-phase fragmentation mechanism of peptides.

2.1. Peptides and Proteins

Proteins are huge organic polymers made up of amino acids. All of the proteins have many important roles such as storage, repair, signalling, structural support, movement, defence mechanism in living cells. Therefore, they are the most abundant (normally % 10-20) substance in the cell after water. Amino acids are the building blocks of peptides and proteins and they are comprising of four major components which are an α-carbon atom, a hydrogen atom, a carboxylic acid group, a primary amine group, and characteristic R group, as shown in Figure 15.

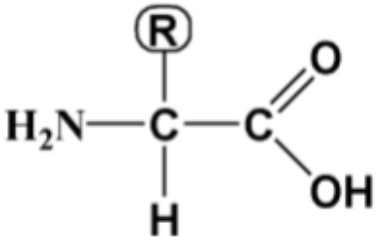

Figure 15. General structure of an amino acid

Physical and chemical characteristic of amino acids depends on the R groups that they have. Amino acids can bond together with a covalent bond (peptide bond) to produce peptide after water elimination. Natural twenty amino acids are shown in Table 1. Common amino acid residues. with all details such as three-letter code, one-letter code.

Table 1. Common amino acid residues

Amino acid name	Three-letter code	One-letter code	Residue Mass (Da)
Glycine	Gly	G	57.021
Alanine	Ala	A	71.037
Serine	Ser	S	87.032
Proline	Pro	P	97.053
Valine	Val	V	99.068
Threonine	Thr	T	101.048
Cysteine	Cys	C	103.009
Isoleucine	Ile	I	113.084
Leucine	Leu	L	113.084
Aspartic Acid	Asp	D	114.027
Asparagine	Asn	N	114.043
Glutamine	Gln	Q	128.059
Lysine	Lys	K	128.095
Glutamic Acid	Glu	E	129.043
Methionine	Met	M	131.040
Histidine	His	H	137.059
Phenylalanine	Phe	F	147.068
Arginine	Arg	R	156.101
Tyrosine	Tyr	Y	163.063
Tryptophan	Trp	W	186.079

All α-carbons (central carbon) of twenty different amino acids have chirality except glycine because it has two same groups (hydrogen). Depending on the difference of R groups, amino acids are basically classified such as non-polar aliphatic (Gly, Ala, Pro, Val, Leu, Ile, and Met), polar uncharged (Ser, Thr, Cys, Asn, and Gln), positively (basic) charged (Lys, His, and Arg), negatively (acidic) charged (Glu and Asp) and aromatic (Phe, Tyr, and Trp).

2.2. Tandem Mass Spectrometry (MS/MS) and Collision-Induced Dissociation (CID)

Amino acid sequence studies are depended on Edman degradation in the past but, it has many limitations like being able to the analysis of peptides having a maximum of 25 amino acids and not suitability for the N-terminal modified peptides. Because of that tandem MS techniques are introduced and then became very famous one for protein chemistry.

In tandem MS there are three stages which are mass selection, mass fragmentation and mass analysis, illustrated in Figure 16.

MS-1 represents the first analyzer and it is responsible for the selection of interest ions. After the selection is completed, selected ions which can be *parent* or *precursor* are fragmentized by collision with inert gas. Helium, argon, xenon, or nitrogen is the most preferred gases for the collision cell. On the other hand, MS-2 represents the second analyzer and it is responsible for obtaining *daughter* ions after the collision. When considering the whole process which consists of generation of the fragment ions by collision is called collision-induced dissociation (CID). Also, in some cases, multi-stage tandem MS is used to get MS^n (n is the number of fragmentation cycle is repeated).

In proteomic studies, the success of obtaining a correct sequence of proteins is the most critical part. Therefore, tandem MS is a breakthrough for proteomics.[23]

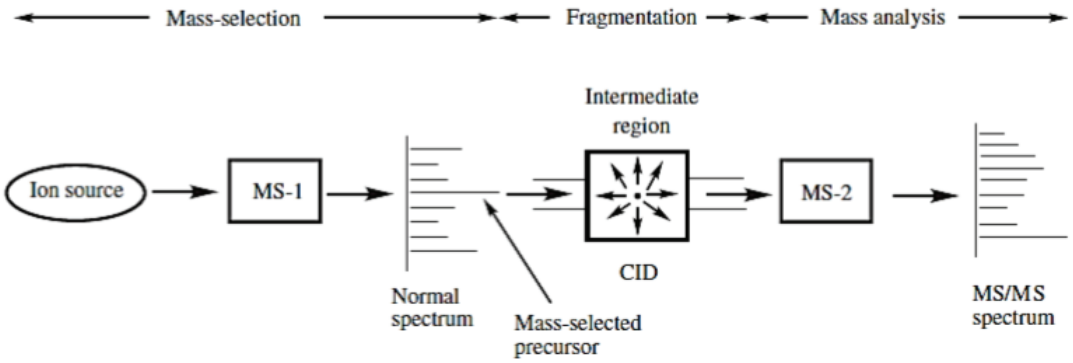

Figure 16. Basic principles of TOF/MS (Source: Dass, et al. 2001)

2.3. Peptide Fragmentation Chemistry

Achieving the sequence of peptides correctly with the help of soft ionization technique is crucial for protein identification. For these studies, structures and pathways of the fragment ions must understand well because obtaining gas-phase peptide fragmentation reaction mechanism is vital for identification of unknown proteins.

2.3.1. Mobile Proton Model

Mobile proton model was defined as a mechanism to understand the fragmentation mechanism of protonated peptides under low-energy CID in the 1990s. Capturing a proton or protons by the peptide in ionization process is the main idea of this model. Location of the captured proton is observed in the most basic side of peptides where are N-terminal amino groups, the side chain of basic amino acids such as His (H), Arg (R) and Lys (K), or amide carbonyl oxygen. When applying CID to the peptides, free proton prefers the thermodynamically less stable site of the peptide backbone. As a conclusion of this movement bond cleavage is takes place between CO and NH (amide bond) and fragment ions which are called charge-directed formation is occurred. In some cases, basic amino acids hold the free proton, so do not allow the peptide to move to the peptide backbone. To overcome this situation, more energy is required.[24-25] Pathways in competition (PIC) mechanism proposed by Paizs and Suhai took its place in the literature in 2005, as shown in Figure 17. PIC mechanism includes charge-directed fragment ions as well as charge-remote fragment ions. Thus, they have improved the perspective of understanding peptide fragmentation routes.[26-27]

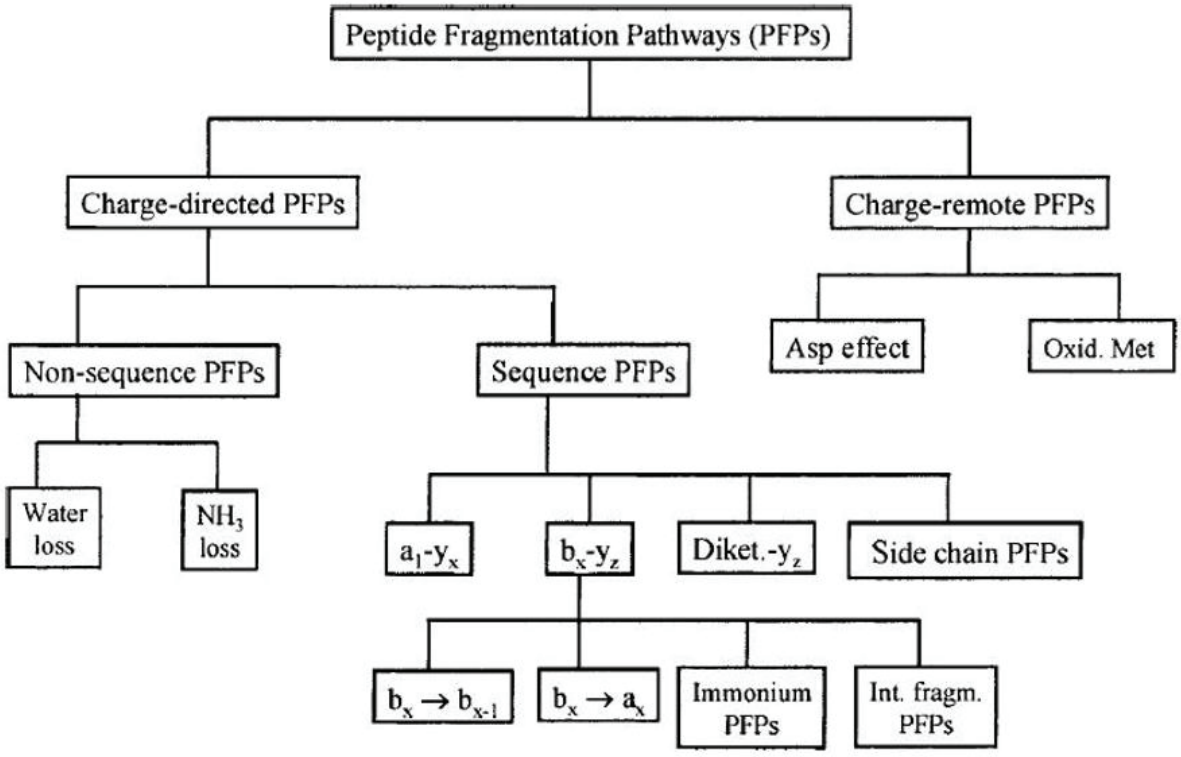

Figure 17. Peptide fragmentation pathways (Source: Paizs, et al. 2005)

2.3.2. Peptide Fragmentation Nomenclature

After proposition of the nomenclature of peptide fragmentation by Roepstrorff & Fohlmann in 1984, Biemann modified it in 1988, as shown Figure 18.[28] When the charge remains on the N-terminal during the bond cleavages via CID, *a*, *b*, or *c* ions are formed. Another option is remaining the charge on the C-terminal which generate *x*, *y*, or *z* ion. There is always a competition between *a* and *x* ions, *b* and *y* ions, *c* and *z* ions based on their proton affinities. Under low-energy CID conditions generally lead to produce *b*, *a* (N-terminal), and *y* (C-terminal) ions. On the other hand, *c* and *z* (cleavage of N-Cα bond) ions are observed under high-energy CID conditions such as electron transfer dissociation (ECD) and electron capture dissociation (ETD).[29]

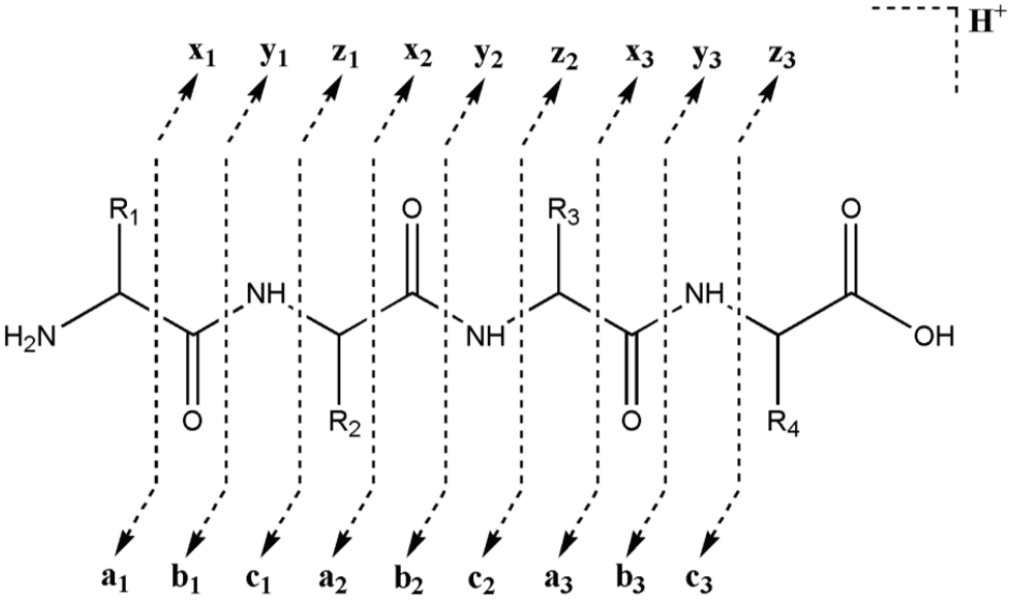

Figure 18. The nomenclature of peptide fragment ions

a ion fragment is formed by elimination of CO (C=O) (carbonyl group). Besides, "°" represents water-loss (-18 Da) and "*" represents ammonia-loss (-17 Da) from fragment ions. Furthermore, the immonium ions ($RCH=NH2^{+}$) can be detected by MS/MS spectrum. Although immonium ions do not describe residues' position in the sequence, they are evidence of certain amino acid residues.[30]

Formation of *b* and *y* ions is crucial for the formation of *a* ions because the elimination of carbonyl group from the *b* ions creates *a* ions as mentioned. Formation of b_3 and y_2 ions from $[M+H]^{+}$ ion of randomly pentapeptide is illustrated in Figure 19. which explains the b_n-y_m pathway (production of N-terminal *b* ions and/or the C-terminal *y* ions).

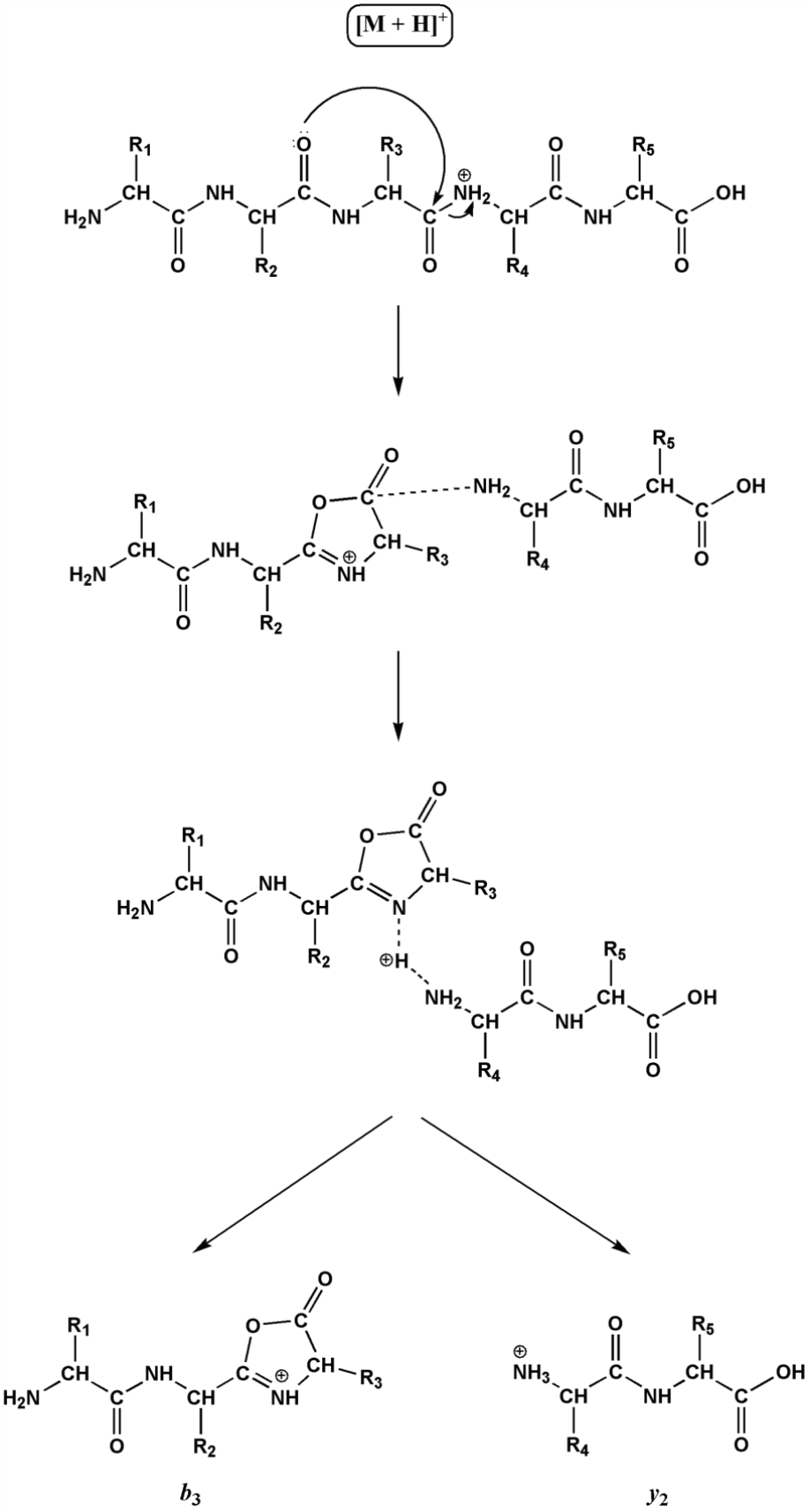

Figure 19. Proposed mechanism for the formation of b_3 and y_2 ions via b_n-y_m pathway

(Source: Mueller et al.1988 and Cordero et al.1993)

2.3.3. Formation of Structure of *b* and *a* ions

In recent years, gas phase reaction and structure of *b* ions have become popular. This tendency is also encouraged to the gas phase reaction and mechanism of *a* ions. Four possible *b* ions structures for b_2, b_3 and b_4 were introduced at the end of 1990s. They were acylium, a diketopiperazine, an oxazolone, and a macrocyclic as shown in Figure 20. The structural difference of *b* ions is affected by the chain length, the amino acid composition which has in sequence and identity of N-terminal amino acid. Firstly (A), thermodynamically stability of an acylium ion is very low. Because of that carbonyl group loss is occurred instantly, so stable iminium ion is formed. Secondly (B), attack of the N-terminal nitrogen atom to the second carbonyl carbon of the protonated amide bond creates a diketopiperazine ion. Thirdly (C), oxazolone structure formation starts with the proton migration to the amide nitrogen and then, N-terminal neighbour amide oxygen attacks to the next C-terminal carbonyl carbon of the protonated amide bond.[27, 31]
Lastly (D), b_5 and bigger than b_5 ions a new structure have been proposed as macrocyclic. After producing the oxazolone ring, N-terminal amine group attack to the carbonyl carbon of the oxazolone ring takes place as shown in Figure 21.[32]

The opening of the macrocyclic ring creates several linear isomers because opening occurs randomly based on the mobile proton. This randomness is also caused of the non-direct sequence and called as sequence scrambling. The ring-opening is a very important step for the gas phase fragmentation studies but, at the same time, it is also caused of the complexity of the mass spectrum which has non-direct and direct sequence ions together.[33-34]

2.3.4. Doubly-Charged Studies in Mass Spectrometry

The discovery of soft ionization techniques and their ability to work with CID has led to the study of gas-phase fragmentation reactions in multiply-protonated ions as well as singly-protonated ions. Although doubly-protonated studies had some limitations, they have contributed greatly to the correct identification of unknown peptide sequences.

Doubly-protonated peptides studies are generally containing *b* and *y* ions which are competitive with each other. Fragmentation pathways of some doubly-charged peptides have basic amino acid residues under low CID were introduced.[35]

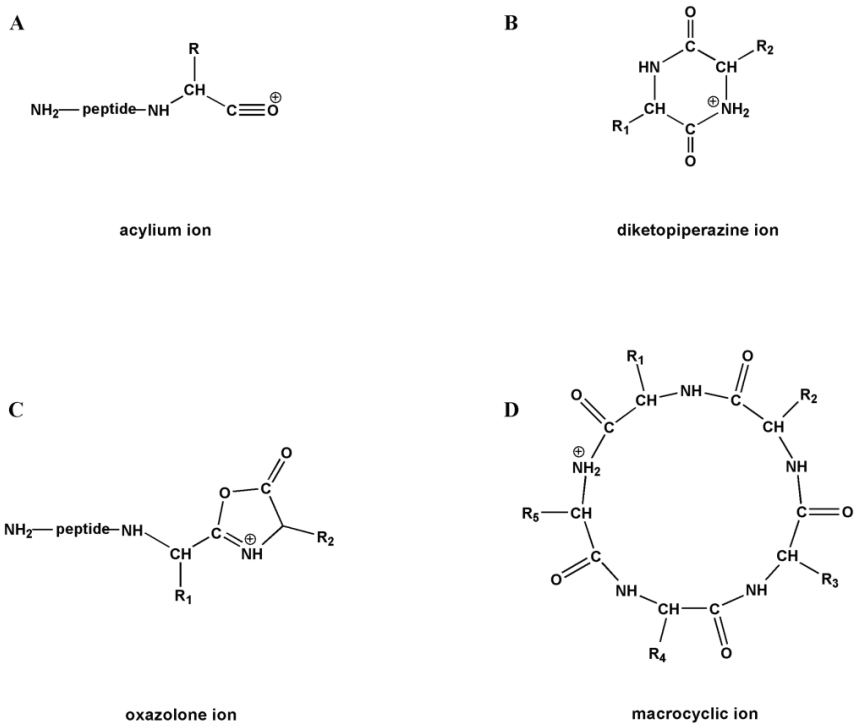

Figure 20. Possible structures for *b* ions

(Source: Yalcin et al. 1996, Paizs et al. 1999, Polce et al. 2000, Paizs and Suhai 2005)

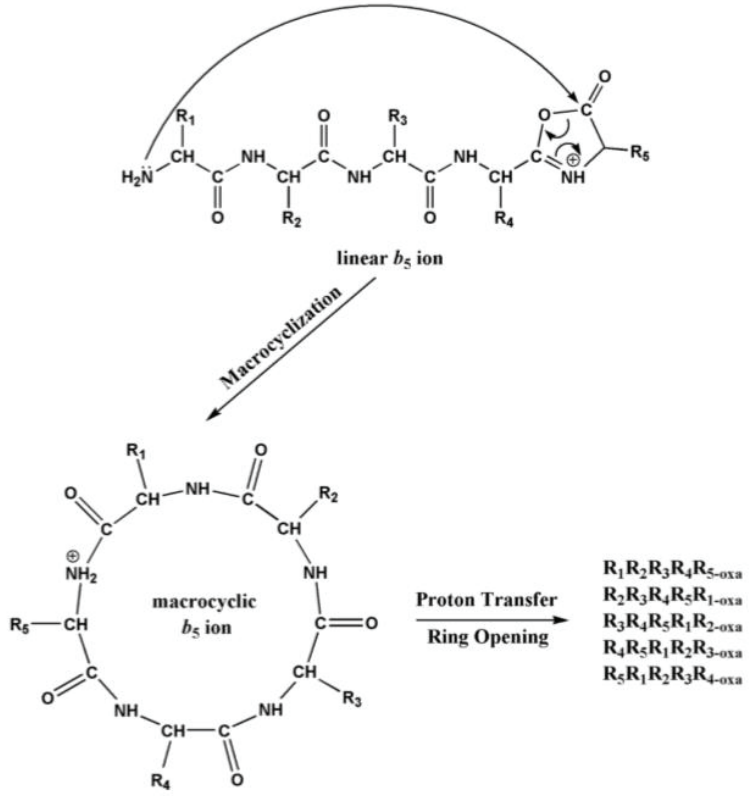

Figure 21. Proposed mechanism for the formation of macrocyclic b_5 ion

(Source: Harrison 2009)

Effect of chain length to the doubly-protonated peptides reactions have been studied (Ala)xHis (x=5, 6, 7, 8, and 10). The complementary ions which are b_2 and y_{N-2} have observed as a major fragmentation reaction in shorter peptides. However, when considering the $(Ala)_{10}His$, major cleavages were observed at the fourth or fifth peptide bond (amide bond). Therefore, the suggested idea was that, chain length effect is crucial for the fragmentation and it supports the bifurcating behaviour.[36]

The first article which has included doubly-protonated b^{2+} ions was published in 2009 by a combination of perfect researchers. In this study, they emphasized the fact that there was more than one path to the fragmentation of b^{2+} ions. First one produces two singly-charged fragments and the other one produces a neutral and doubly-protonated fragment as shown in Figure 22. (as-DPD = asymmetric doubly-protonated dimers) (s-DPD = symmetric doubly-protonated dimers).[37]

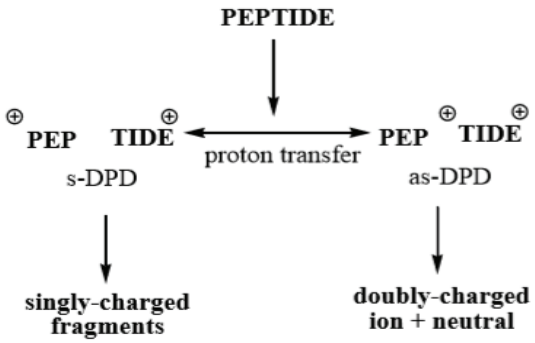

Figure 22. Routes of fragmentation of doubly-protonated peptides

(Source:Young, et al 2009)

In 2009, a_2^{2+} from Pro-Pro (Diproline) and a_3^{2+} from Pro-Pro-Pro (Triproline) peptides were published. They suggested that, $(a_2 + H)^{2+}$ ion can be generated from $(a_3 + H)^{2+}$ ion and they supported this conclusion with DFT calculations

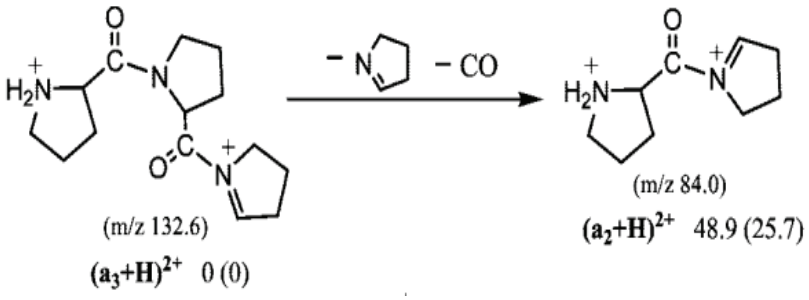

Figure 23. Fragmentation of $(a_3 + H)^{2+}$ (Source: Hopkinson, et al. 2011)

Another research related with the doubly protonated *a* ions was introduced in 2011, but they also studied other peptides which have Pro and Gly, Leu, Val or Met residues. For example, $(a_3 + H)^{2+}$ was observed from Pro-Gly-Gly peptides and the other positions of Pro. After all CID and computational experiments they suggested that, regardless of Pro position, it has a great effect for generating $(a_3 + H)^{2+}$ ions.[38]

Also, different types of multiply-charged studies were published in the literature. By using $[La(peptide)]^{3+}$ complexes, it was discovered which peptide could form complex. According to the earlier has phase studies, tripositively charged metal ions could not bond to the small peptides very well. In this work suggested that, peptides which have including one or more than one arginine residues can make complexes based on the delocalization of the positive charge in arginine.[39]

2.4. Aim of the Thesis

An understanding amino acid sequence of peptides correctly is a huge and crucial work area because it is directly related to human health. A living organism generates many kinds of proteins under different conditions such as stress, illness, unhappiness or even health and happiness. Identifying these kinds of proteins and their sequences is the keystone of producing or inhibiting them.

In the last decades, gas-phase fragmentation reactions of singly-protonated and doubly-protonated have become very famous to understanding the structure and behavior of fragment ions. When considering the contents of studies, singly-protonated works are more than doubly-protonated.

In this work, we determined to investigate the fragmentation reactions of doubly-protonated *a* ions derived from model peptides which have basic amino acid. All basic amino acids (Arginine, Lysine and Histidine) because of the ability to hold one proton on their side chain were studied to examine doubly-charged macrocyclic behavior of a_7^{2+} ions. As mentioned, three sets of model peptides were used to understand the structure and behaviors of a_7^{2+} ions in detail.

CHAPTER 3

EXPERIMENTAL

Three sets of C-terminal amidated model peptides HAAAAAA-NH_2, AHAAAAA-NH_2, AAHAAAA-NH_2, AAAHAAA-NH_2, AAAAHAA-NH_2, AAAAAHA-NH_2, AAAAAAH-NH_2, RAAAAAA-NH_2, ARAAAAA-NH_2, AARAAAA-NH_2, AAARAAA-NH_2, AAAARAA-NH_2, AAAAARA-NH_2, AAAAAAR-NH_2, and KAAAAAA-NH_2, AKAAAAA-NH_2, AAKAAAA-NH_2, AAAKAAA-NH_2, AAAAKAA-NH_2, AAAAAKA-NH_2, AAAAAAK-NH_2, HYAGFLV-NH_2, YAGHFLV-NH_2, YAGFLVH-NH_2, KYAGFLV-NH_2, YAGKFLV-NH_2, YAGFLVK-NH_2, RYAGFLV-NH_2, YAGRFLV-NH_2 and YAGFLVR-NH_2 were purchased from GL Biochem Ltd. (Shanghai, China) Stock solution with a 10^{-2} or 10^{-4} M was prepared by dissolving of a 1-1.5 mg of each solid model peptide in 1:1 (v/v) CH_3OH:H_2O. Then they were diluted by 1:1 (v/v) CH_3OH:H_2O and 1% formic acid to obtain micromolar concentration.

LTQXL linear ion-trap mass spectrometer (Thermo Finnigan, San Jose, CA, USA) equipped with an ESI source was used for all multistage mass spectrometry (MS^n) experiments. The instrument was calibrated with the company's calibration mixture (Calmix: caffeine, MRFA, and Ultramark) before each experiment. All the experimental settings such as voltage, lens, multipole, offset etc. were optimized to obtain maximum $[M+2H]^{2+}$ ion peak with the LTQ Tune software. The ion spray voltage was always + 5.00 kV and the nitrogen as a sheet gas flow rate was 8 or 7 arbitrary units. (au) For improving trapping efficiency, helium gas was used as collision gas. Normalized collision energy determined at between 16-24 % with activation (q) of 0.250, and activation time of 30 ms was applied at each CID stage. For all precursor and daughter ions, isolation width (*m/z*) was set at between 1.5 - 2.5. After introducing a 100 μM each peptide solution with 5 μL/min flow rate, at least 500 scans were averaged with a scan rate of 1 employed.

CHAPTER 4

RESULTS AND DISCUSSIONS

4.1. Introduction

To understanding gas-phase fragmentation behavior of *b* and also *a* ions have vital importance in protein chemistry. Tryptic digestion method is a very common technique to obtain peptides from proteins at the literature and trypsin enzyme is a specific enzyme which cut the proteins at a specific point generating C-terminal Arg (R) and Lys (K) positioned peptides. These amino acids are very basic and available to be multiply-protonated

From another point of view, His (H) is the third most basic amino acid existed in nature. Therefore, there have been lots of studies about gas-phase fragmentation behavior of His containing peptides. Observation from more than 500 different tryptic peptides explained that His effects the enhancement of cleavage in doubly-protonated tryptic peptides as an internal amino acid.[40]

Based upon these researches His, Arg and Lys residues were used for creating doubly-charged a_7 ion. Basic amino acids were pointed in AAAAAA-NH_2 series which has less reactive features from N-terminal to C-terminal, and YAGFLV-NH_2 series which are popular for our research area.

In conclusion, in our study CID of MS^4 behavior of fragment a_7 ions in doubly-protonated peptides were investigated. The results were explained in the following sections in detail.

4.2. Investigation of Macrocyclic Behavior of Doubly-Protonated a_7 Ions

As evidence of macrocyclization, the formation of non-direct sequence ions in the MS/MS spectra of doubly-protonated *a* ions can be shown. In this part of the thesis, to investigate the macrocyclic behavior of a_7^{2+} ion (MS/MS/MS/MS spectra) upon CID is aimed. The AAAAAA-NH_2 peptide sequence motif was used because the fragmentation characteristics of this sequence have been well studied from our group. Besides,

YAGFLV-NH_2 peptide series were used to compare similarities and differences of macrocyclic behavior of basic amino acid containing residues between C-terminal amidated YAGFLV and AAAAAA series.

4.2.1. His Residue Containing AAAAAA-NH_2 Peptide Series

In the first section, CID of a_7^{2+} (m/z 268.5) of HAAAAAA-NH2, AHAAAAA-NH_2, AAHAAAA-NH_2, AAAHAAA-NH_2, AAAAHAA-NH_2, AAAAAHA-NH_2, AAAAAAH-NH_2 (MS4) were performed. This series of peptides have an ability to compare with the other series containing basic amino acid.

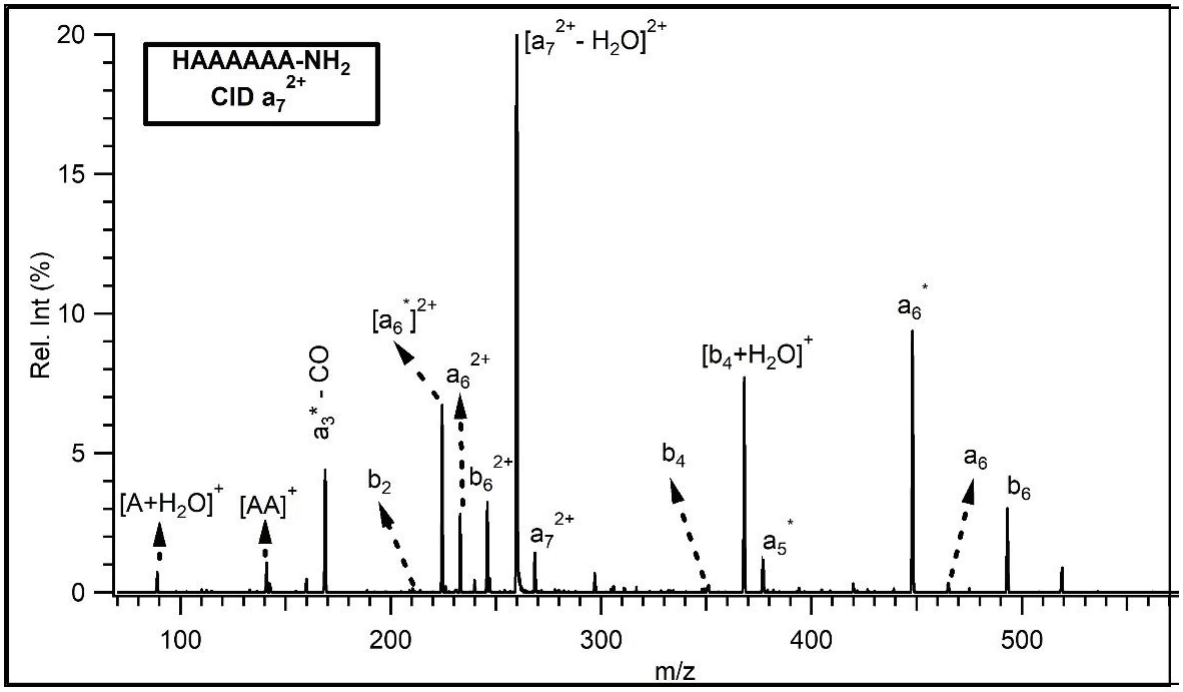

Figure 24. CID mass spectrum of a_7^{2+} ion of HAAAAAA-NH_2

Initially, His residue was positioned at the N-terminal of AAAAAA-NH_2 heptapeptides. In Figure 24, doubly-protonated a_7 ion CID mass spectrum of HAAAAAA-NH_2 was examined. The peak at *m/z* 259.92 was observed as water (H_2O) elimination from a_7^{2+} (*m/z* 268.42). In addition to this, b_6^{2+} (*m/z* 245.75), a_6^{2+} (*m/z* 232.92), $[a_6^*]^{2+}$ (*m/z* 224.25) ions were observed as a doubly-protonated. On the other hand, $[AAA]^*$ - CO (*m/z* 168.67), $[AA]^+$ (*m/z* 141.0), $[A+H_2O]^+$ (*m/z* 89.0), b_6 (*m/z* 493), a_6^* (*m/z* 447.48), a_5^* (*m/z* 376.83), $[b_4+H_2O]^+$ (*m/z* 367.75), b_4 (*m/z* 249.08) fragmentations were observed singly-protonated under low energy CID conditions.

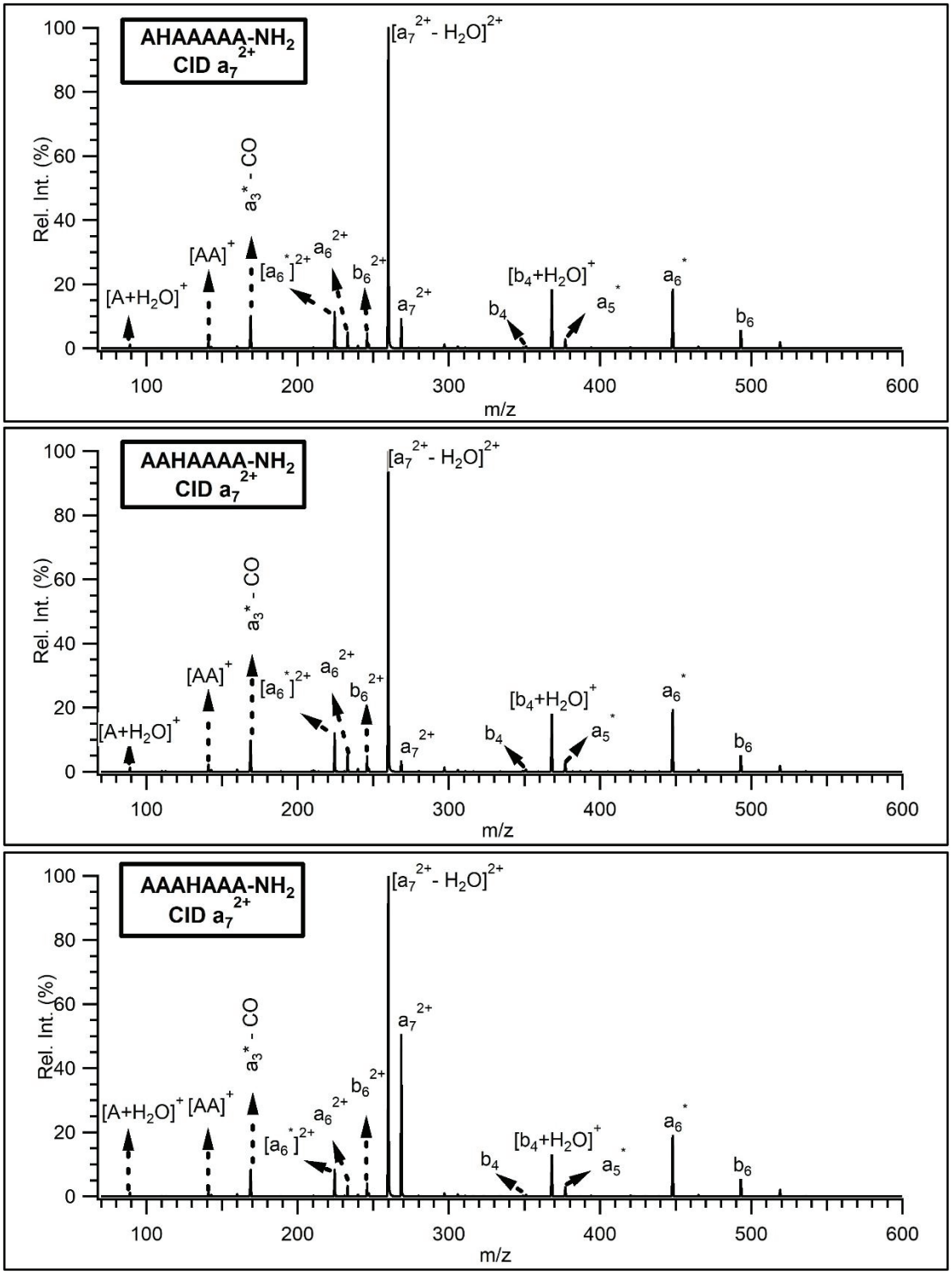

Figure 25. Comparison of a_7^{2+} ion CID mass spectra of AHAAAAA-NH_2, AAHAAAA-NH_2 and AAAHAAA-NH_2

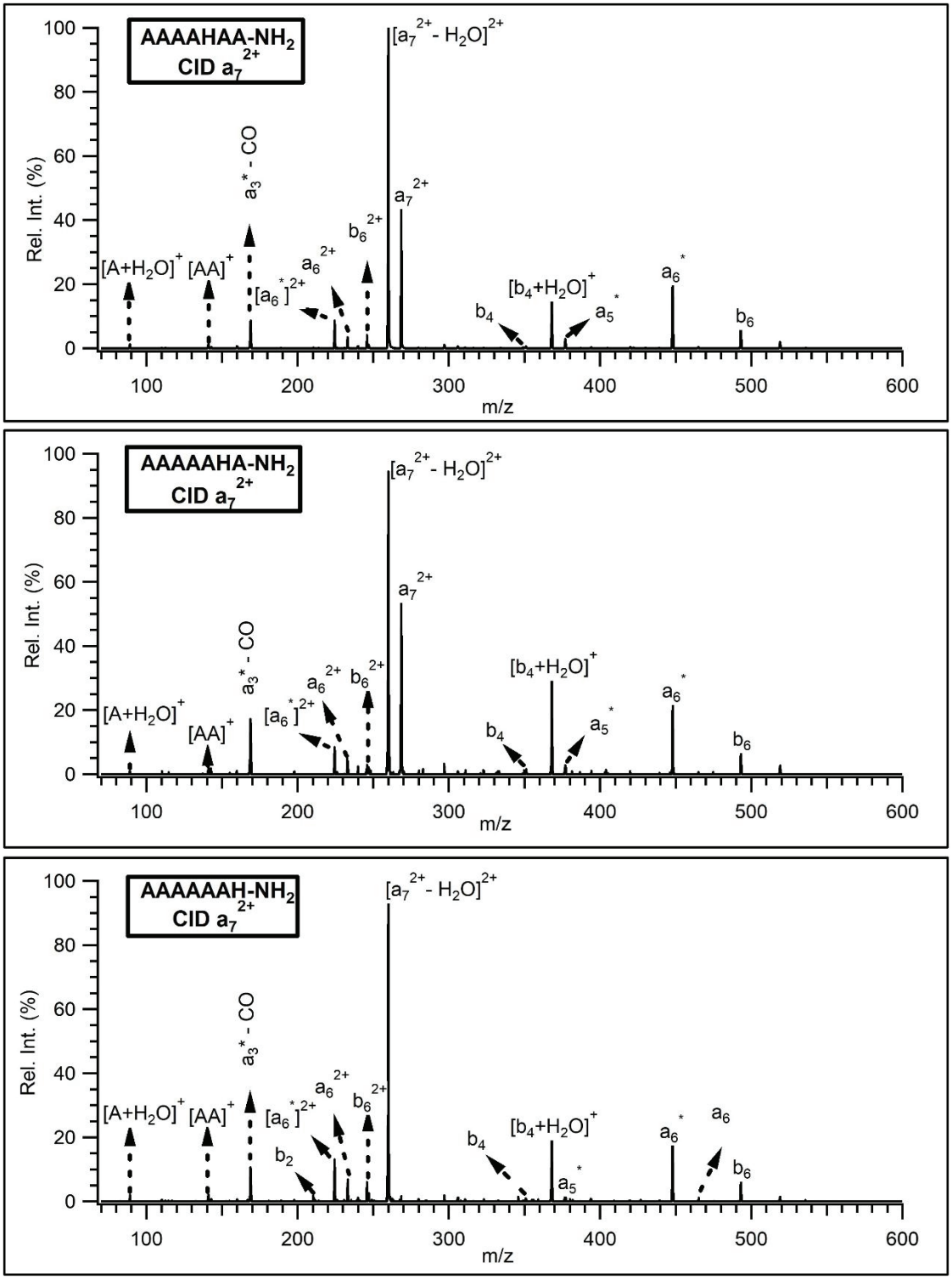

Figure 26. Comparison of a_7^{2+} ion CID mass spectra of AAAAHAA-NH_2, AAAAAHA-NH_2 and AAAAAH-NH_2

Figure 25 and Figure 26 shows that the fragmentation patterns of the m/z 268.42 ions derived from C-terminal amidated Ala containing heptapeptides (AHAAAAA-NH_2, AAHAAAA-NH_2, AAAHAAA-NH_2, AAAAHAA-NH_2, AAAAAHA-NH_2 and AAAAAAH-NH_2) demonstrates entirely the same product ions in their CID mass spectra and the most intense fragment ion is $[a_7^{2+}+H_2O]^{2+}$ (*m/z* 259.92) for all of them.

The same observation of all spectrum and observation of fragmentation ions a_7^{2+} (*m/z* 268.42), b_6^{2+} (*m/z* 245.75), a_6^{2+} (*m/z* 232.92) $[AA]^+$ (*m/z* 141.0) and $[A+H_2O]^+$ (*m/z* 89.0) which are non-direct sequence ions. They are the evidence of macrocyclization.

4.2.2. Lys Residue Containing AAAAAA-NH_2 Peptide Series

In the second section, CID of a_7^{2+} (m/z 264.08) of KAAAAAA-NH_2, AKAAAAA-NH_2, AAKAAAA-NH_2, AAAKAAA-NH_2, AAAAKAA-NH_2, AAAAAKA-NH_2, AAAAAAK-NH_2 (MS^4) were performed. This series of peptides have an ability to compare with the other series containing basic amino acid again.

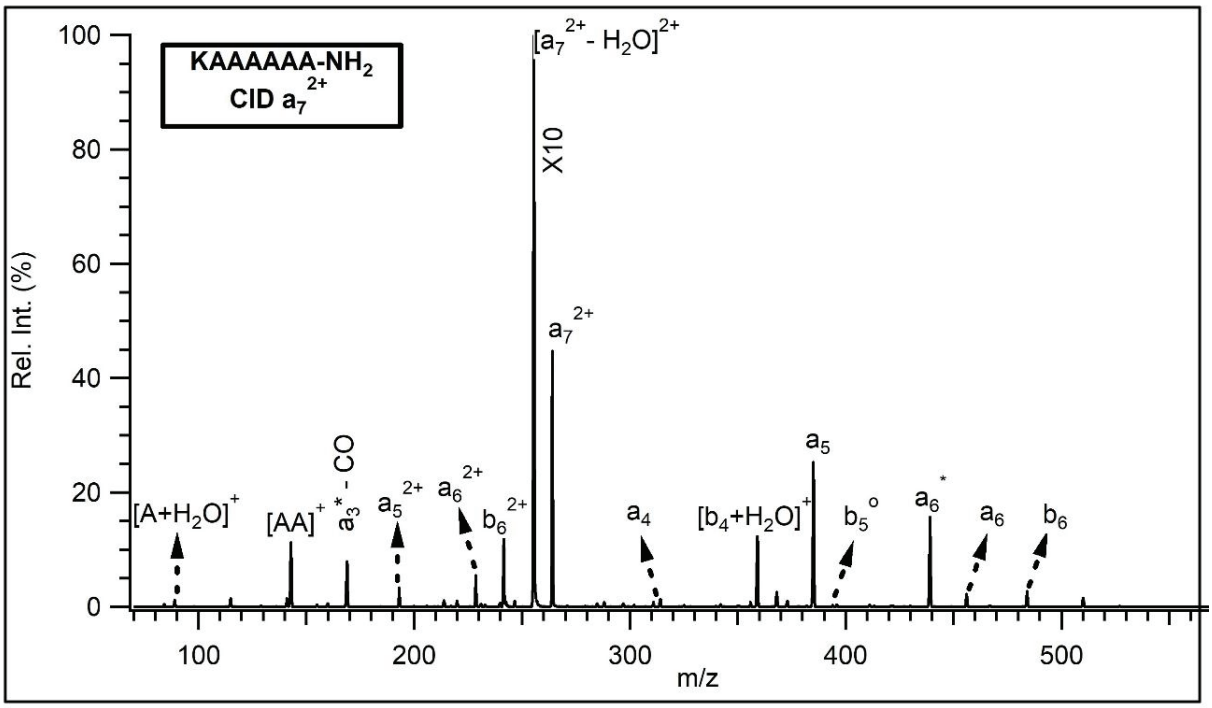

Figure 27. CID mass spectrum of a_7^{2+} ion of KAAAAAA-NH_2

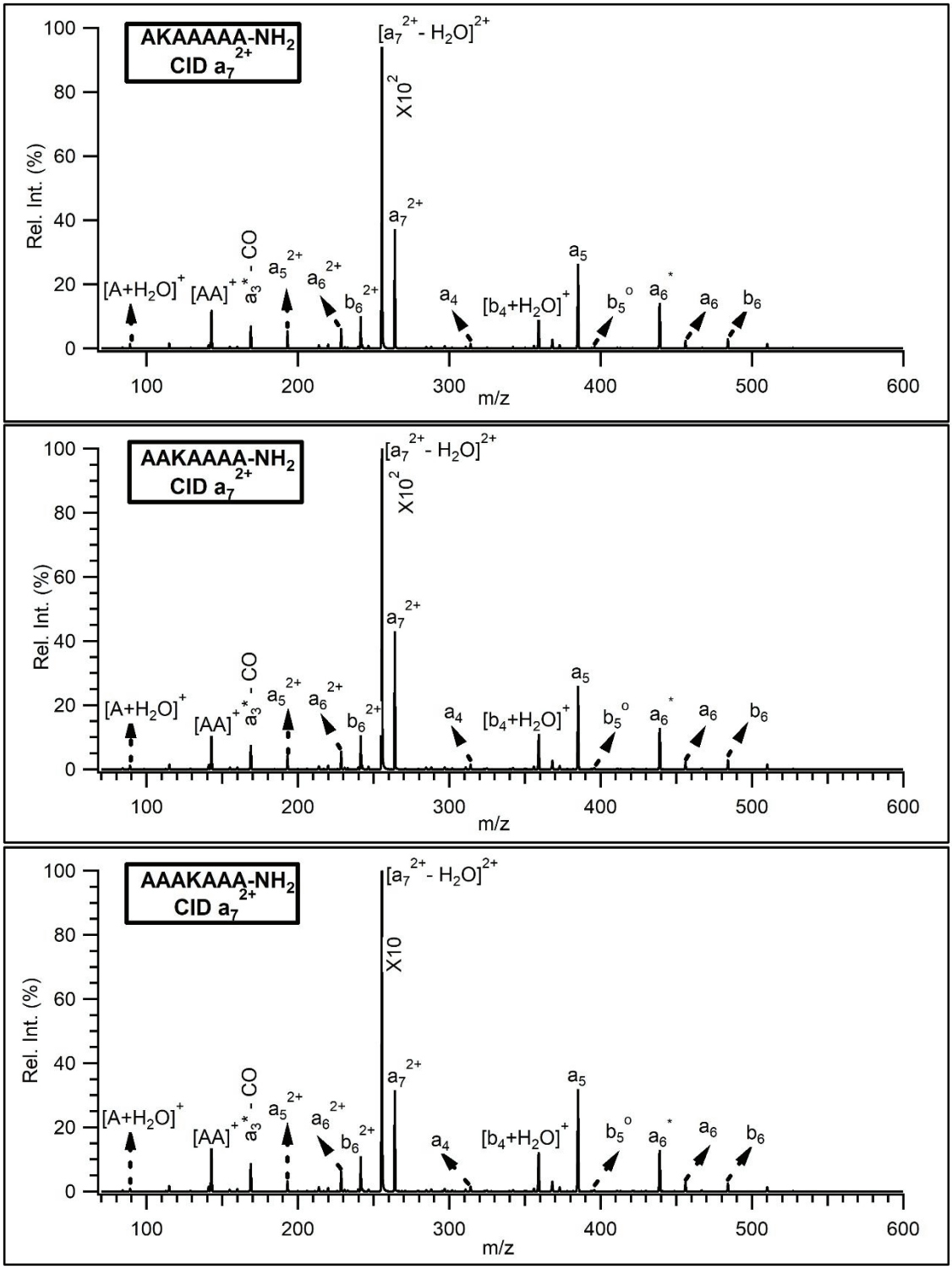

Figure 28. Comparison of a_7^{2+} ion CID mass spectra of AKAAAAA-NH_2, AAKAAAA-NH_2 and AAAKAAA-NH_2

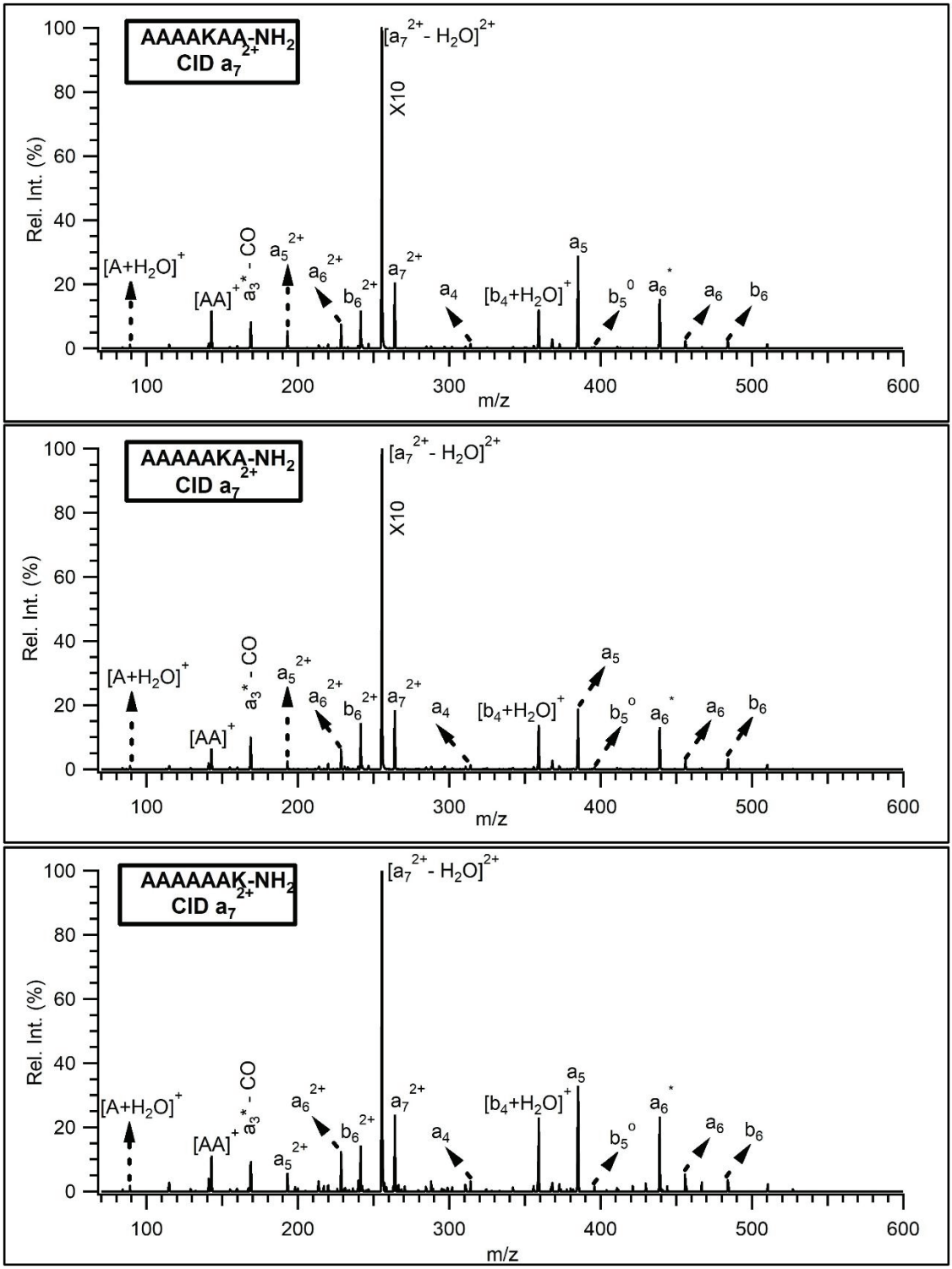

Figure 29. Comparison of a_7^{2+} ion CID mass spectra of AAAAKAA-NH_2, AAAAAKA-NH_2 and AAAAAK-NH_2

At this part of the study, Lys residue was positioned at the N-terminal of AAAAAA-NH_2 heptapeptides. In Figure 27, doubly-protonated a_7 ion CID mass spectrum of KAAAAAA-NH_2 was examined. The peak at *m/z* 255.25 was observed as water (H_2O) elimination from a_7^{2+} (*m/z* 264.0). In addition to this, b_6^{2+} (*m/z* 241.33), a_6^{2+}(*m/z* 228.42), $[a_5]^{2+}$ (*m/z* 193.0) ions were observed as a doubly-protonated. On the other hand, $[AAA]^*$ - CO (*m/z* 168.67), $[AA]^+$ (*m/z* 141.75), $[A+H_2O]^+$ (*m/z* 89.0), b_6 (*m/z* 484.0), a_6 (*m/z* 456.02) a_6^* (*m/z* 438.02), a_5 (*m/z* 385.0), $[b_4+H_2O]^+$ (*m/z* 358.92), a_4 (*m/z* 314.0) fragmentations were observed singly-protonated under low energy CID conditions.

Figure 28 and Figure 29 shows that the fragmentation patterns of the m/z 264.0 ions derived from C-terminal amidated Ala containing heptapeptides (AKAAAAA-NH_2, AAKAAAA-NH_2, AAAKAAA-NH_2, AAAAKAA-NH_2, AAAAAKA-NH_2 and AAAAAAK-NH_2) demonstrates entirely the same product ions in their CID mass spectra and the most intense fragment ion is $[a_7^{2+}+H_2O]^{2+}$ (*m/z* 255.25) for all of them.

Fragmentation ions b_6 (*m/z* 484.0), a_6 (*m/z* 456.02), a_5 (*m/z* 385.0), b_6^{2+} (*m/z* 241.33) a_6^{2+} (*m/z* 228.42), $[AA]^+$ (*m/z* 141.75) and $[A+H_2O]^+$ (*m/z* 89.0) which are non-direct sequence. Moreover, this fact also an evidence of macrocyclization again.

When compared with the His residue, differences were observed in some doubly-protonated and singly-protonated fragmentations. His and Lys have different basicity, molecular weight and structure so these facts affect the fragmentations differently.

4.2.3. Arg Residue Containing AAAAAA-NH_2 Peptide Series

In the third section, CID of a_7^{2+} (m/z 278.08) of RAAAAAA-NH_2, ARAAAAA-NH_2, AARAAAA-NH_2, AAARAAA-NH_2, AAAARAA-NH_2, AAAAARA-NH_2, AAAAAAR-NH_2 (MS^4) were performed. This series of peptides have an ability to compare with the other series containing basic amino acid again.

At the Arg base study, Arg residue was positioned at the N-terminal of AAAAAA-NH_2 heptapeptides. In Figure 30, doubly-protonated a_7 ion CID mass spectrum of RAAAAAA-NH_2 was examined. The peak at *m/z* 269.42 was observed as water (H_2O) elimination from a_7^{2+} (*m/z* 278.0). Furthermore, b_6^{2+} (*m/z* 255.33), a_6^{2+} (*m/z* 242.42), $[a_6^*]^{2+}$ (*m/z* 233.83) ions were observed as a doubly-protonated. The other fragmentations $[AAA]^*$ - CO (*m/z* 168.67), $[AA]^+$ (*m/z* 141.75), $[A+H_2O]^+$ (*m/z* 89.0), b_6 (*m/z* 512.0), a_6 (*m/z* 483.92), $[a_6\text{-}H_2O^+]$ (*m/z* 467.0), b_5 (*m/z* 440.75), $[b_4+H_2O]^+$ (*m/z* 387.92), b_4 (*m/z*

370.0), $[b_3+H_2O]^+$ (*m/z* 316.0) were observed singly-protonated under low energy CID conditions.

Figure 31 and Figure 32 shows that the fragmentation patterns of the m/z 278.0 ions derived from C-terminal amidated Ala containing heptapeptides (ARAAAAA-NH_2, AARAAAA-NH_2, AAARAAA-NH_2, AAAARAA-NH_2, AAAAARA-NH_2 and AAAAAAR-NH_2) demonstrates entirely the same product ions in their CID mass spectra and the most intense fragment ion is $[a_7^{2+}+H_2O]^{2+}$ (*m/z* 269.42) for all of them.

Evidence of macrocyclization are that b_6 (*m/z* 512.0), a_6 (*m/z* 483.92), b_5 (*m/z* 440.75), b_4 (*m/z* 370.0), b_6^{2+} (*m/z* 255.33) a_6^{2+} (*m/z* 242.42), $[AA]^+$ (*m/z* 141.75) and $[A+H_2O]^+$ (*m/z* 89.0) fragments are non-direct sequence ions.

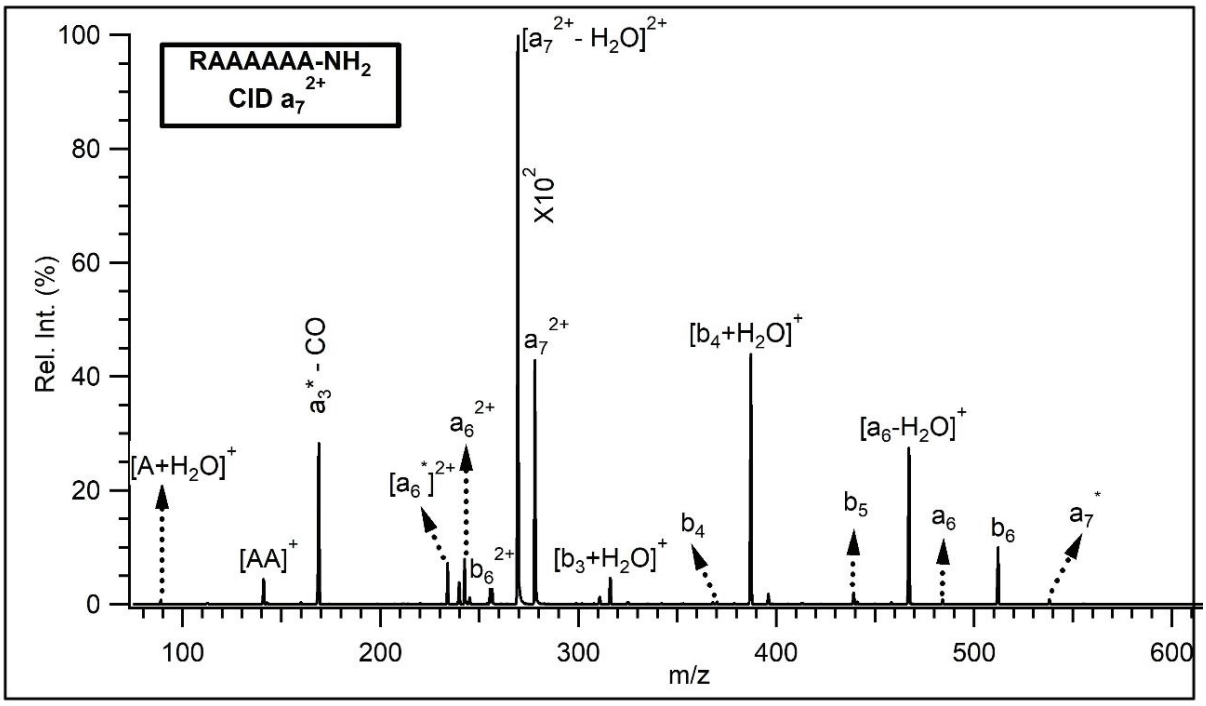

Figure 30. CID mass spectrum of a_7^{2+} ion of RAAAAAA-NH_2

Based upon the whole mass spectra of AAAAAA-NH_2 series which containing His, Lys and Arg residue at all positions from N-terminal to the C-terminal a new mechanism was proposed. The fragmentation reaction mechanism of $[M+2H]^{2+}$ ion of AAAHAAA-NH_2 are shown in Figure 33. AAAHAAA-NH_2 peptide was chosen as an example for explaining the mechanism.

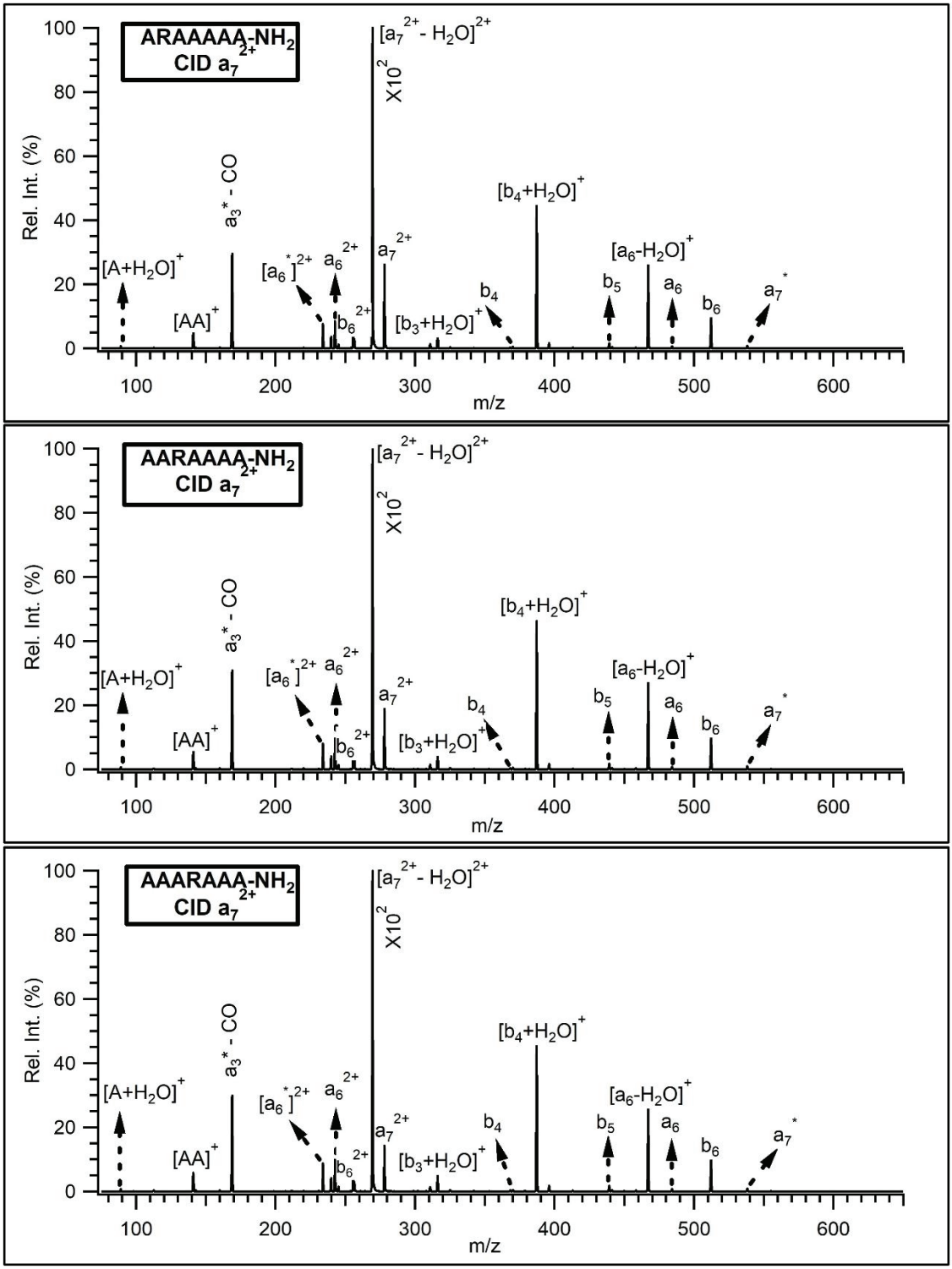

Figure 31. Comparison of a_7^{2+} ion CID mass spectra of ARAAAAA-NH_2, AARAAAA-NH_2 and AAARAAA-NH_2

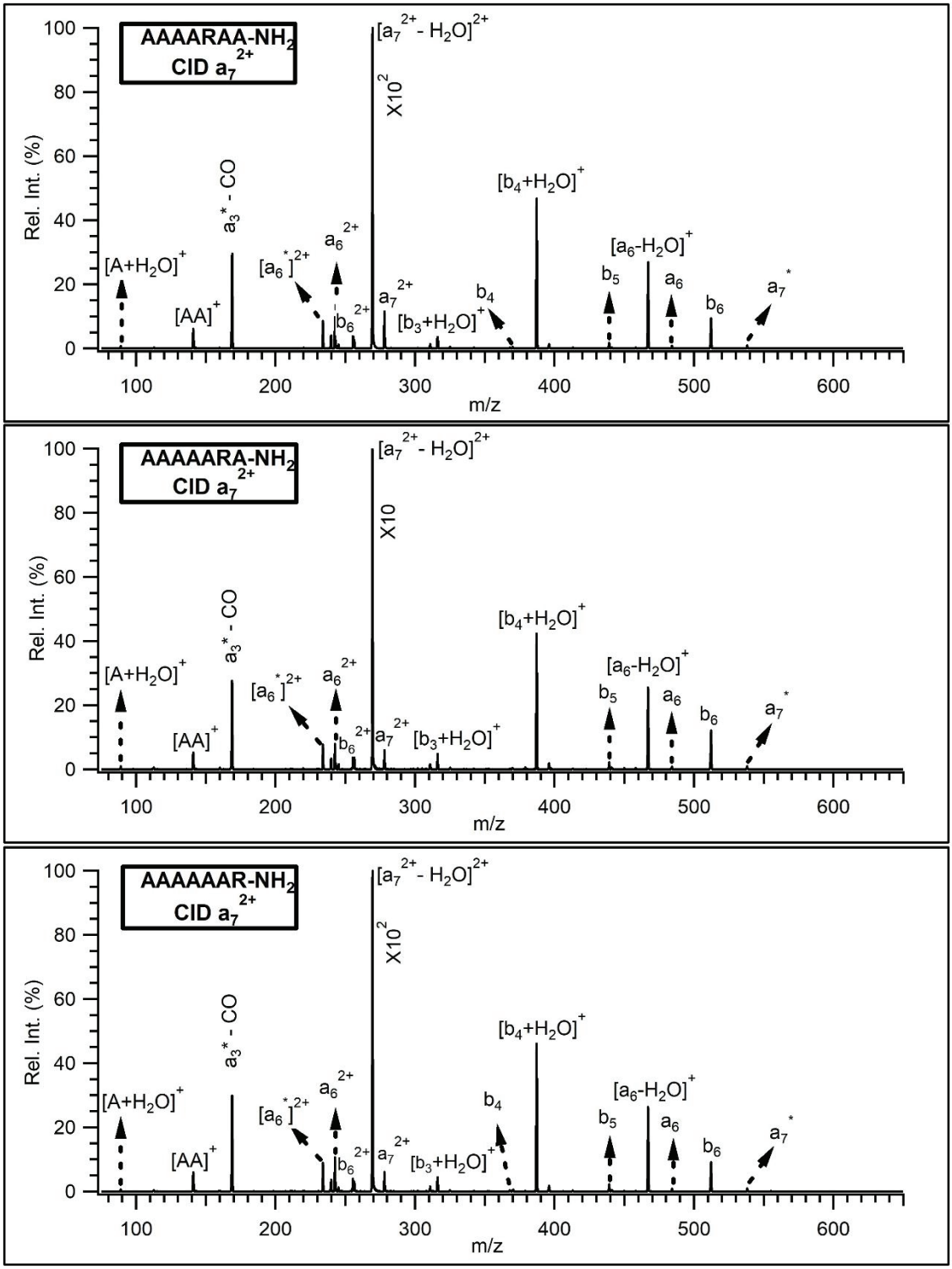

Figure 32. Comparison of a_7^{2+} ion CID mass spectra of AAAARAA-NH_2, AAAAARA-NH_2 and AAAAAAR-NH_2

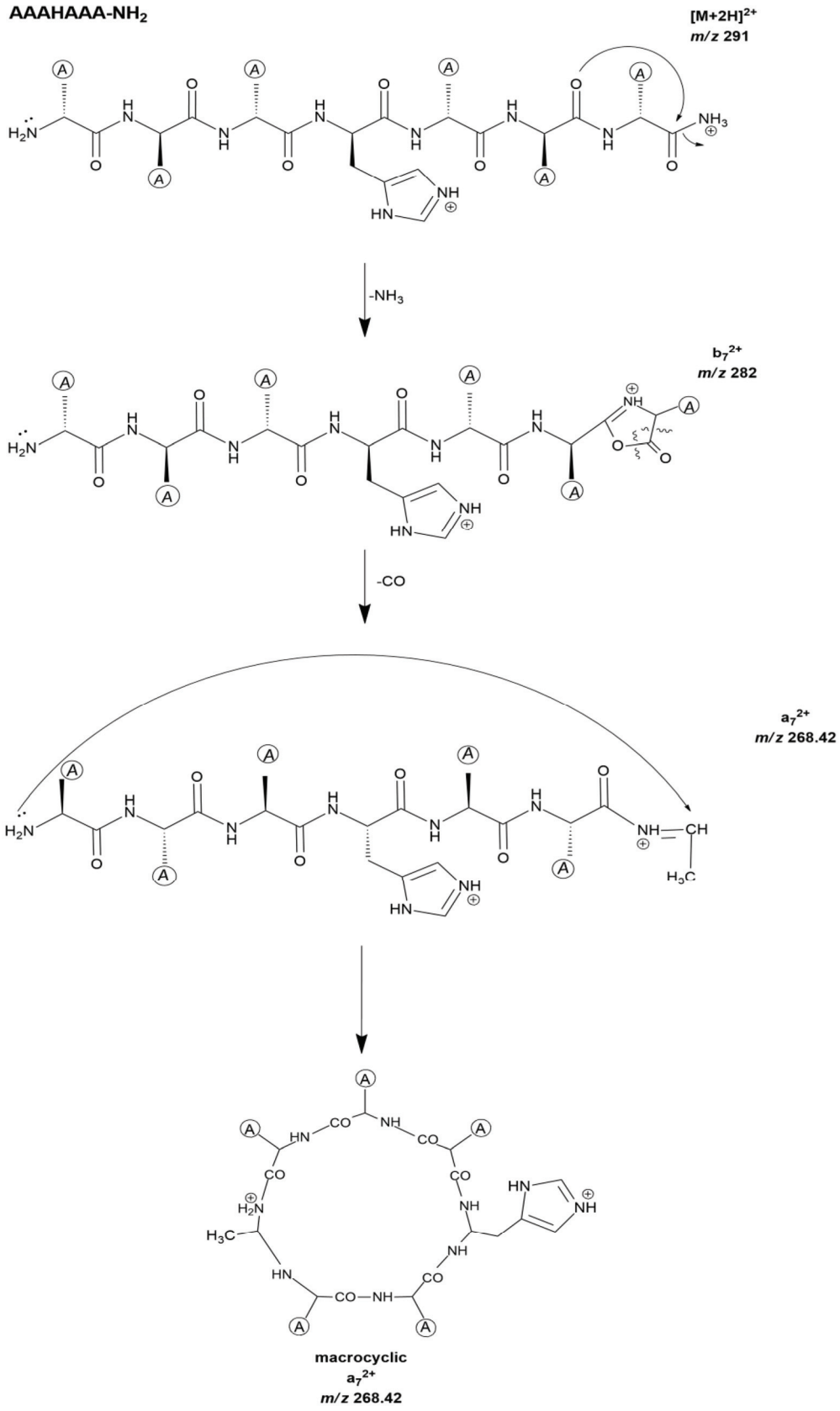

Figure 33. Proposed reaction mechanism for the formation of macrocyclic a_7^{2+} ion in the gas-phase

The first structure indicates a doubly-protonated form of AAAHAAA-NH_2 at *m/z* 291.0 where z equals to two. The first proton is positioned to the side chain of His residue while the second proton is located at the C-terminal amine group.

Afterward, the ammonia is lost (-17 Da) from $[M+2H]^{2+}$ ion via nucleophilic attack of carbonyl oxygen to the next carbonyl carbon which then leads to the formation of protonated five-membered oxazolone ring at the C-terminal end of the peptide. Doubly-protonated b_7^{2+} ion was generated. Then, loss of (-14 Da) [CO] from b_7^{2+} occurred and this situation creates a_7^{2+} ion.

Finally, the generated doubly-protonated a_7^{2+} ion undergoes macrocyclization reaction in the gas-phase. The macrocyclic structure may undergo numerous ring-opening pathways to form seven different a_7^{2+} isomers.

On the other hand, the formation of macrocyclic b_6^+ ion was also proposed. After the a_7^{2+} was generated, Unpaired electrons of NH_2 from the N-terminal can attack to the carbonyl group which is adjacent of NH^+ at the C-terminal. Therefore, macrocyclic b_6^+ can be formed. (Figure 34)

Considering the all AAAAAA-NH_2 series, all spectrums had same a_3^* -CO (*m/z* 168.67) peak (Figure 35). It includes only Alanine fragmentation because of that, the peak was also examined, and a mechanism was proposed for formation. (Figure 36)

4.3. His, Lys and Arg Residue Containing YAGFLV-NH_2 Peptide Series

After finding a same a_3^* - CO (*m/z* 168.67) peak for all of Ala residues, in this part, CID of a_7^{2+} of HYAGFLV-NH_2, YAGHFLV-NH_2 and YAGFLVH- NH_2, KYAGFLV-NH_2, YAGKFLV-NH_2, YAGFLVK-NH_2, RYAGFLV-NH_2, YAGRFLV-NH_2 and YAGFLVR- NH_2 heptapeptides were performed to find the same peak for all of them again.

4.3.1. His Residue Containing YAGFLV-NH_2 Peptide Series

Firstly, in Figure 37, doubly-protonated a_7 ion CID mass spectrum of HYAGFLV-NH_2, was examined. The signal of a_7^{2+} ion was too low, so spectrum is not so clear. However, a_7^{+2} (*m/z* 380.5), a_7^{+2}- NH_3 (*m/z* 372.0), a_7^{+2}- (CO+NH_3) (*m/z* 358.0), a_7^{+2}- (Glycine+NH_3) (*m/z* 343.5), F_{imm} (*m/z* 120.0) and Y_{imm} (*m/z* 136.0) non-direct sequences

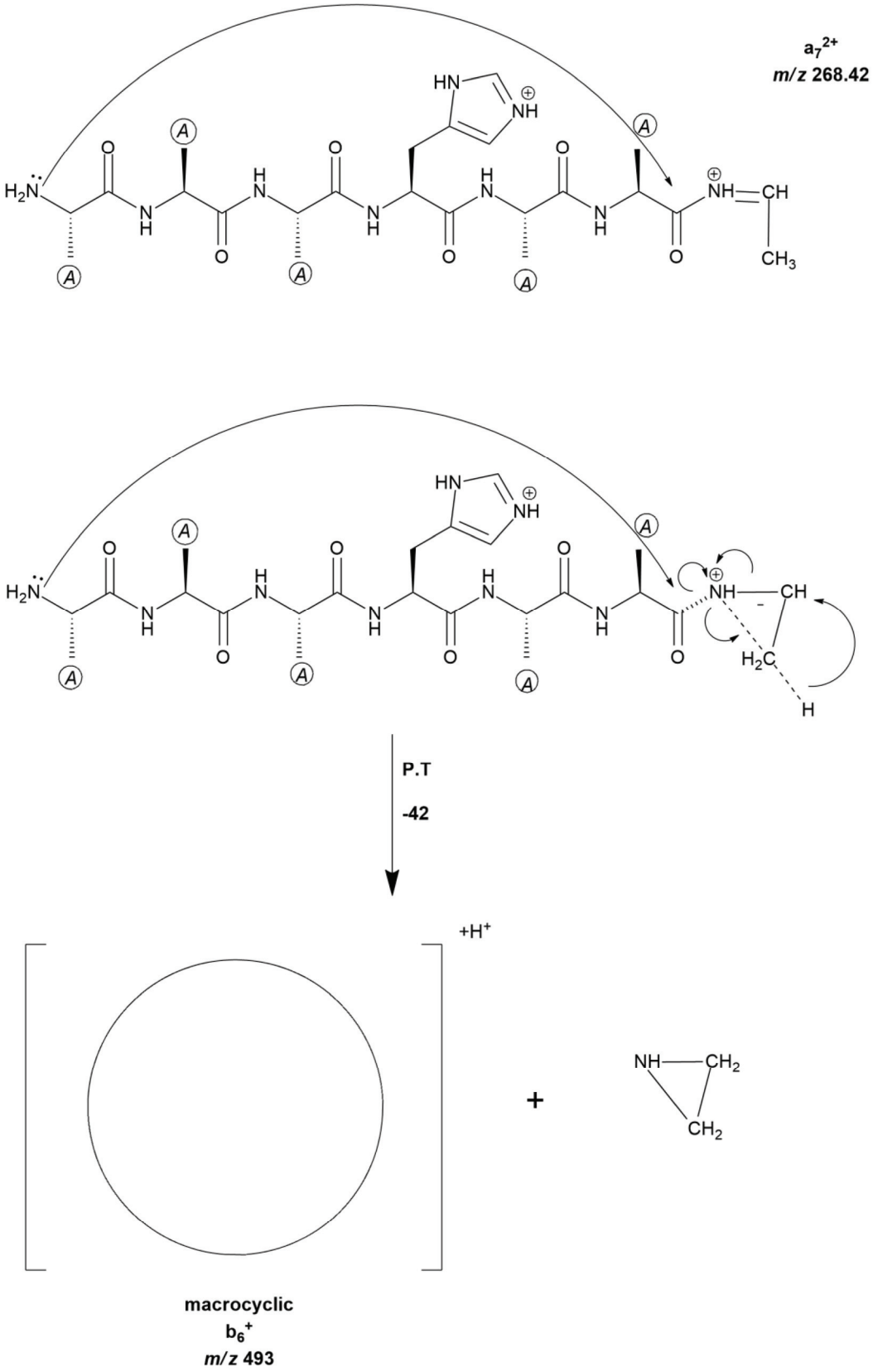

Figure 34. Proposed reaction mechanism for the formation of macrocyclic b_6^+ ion in the gas-phase

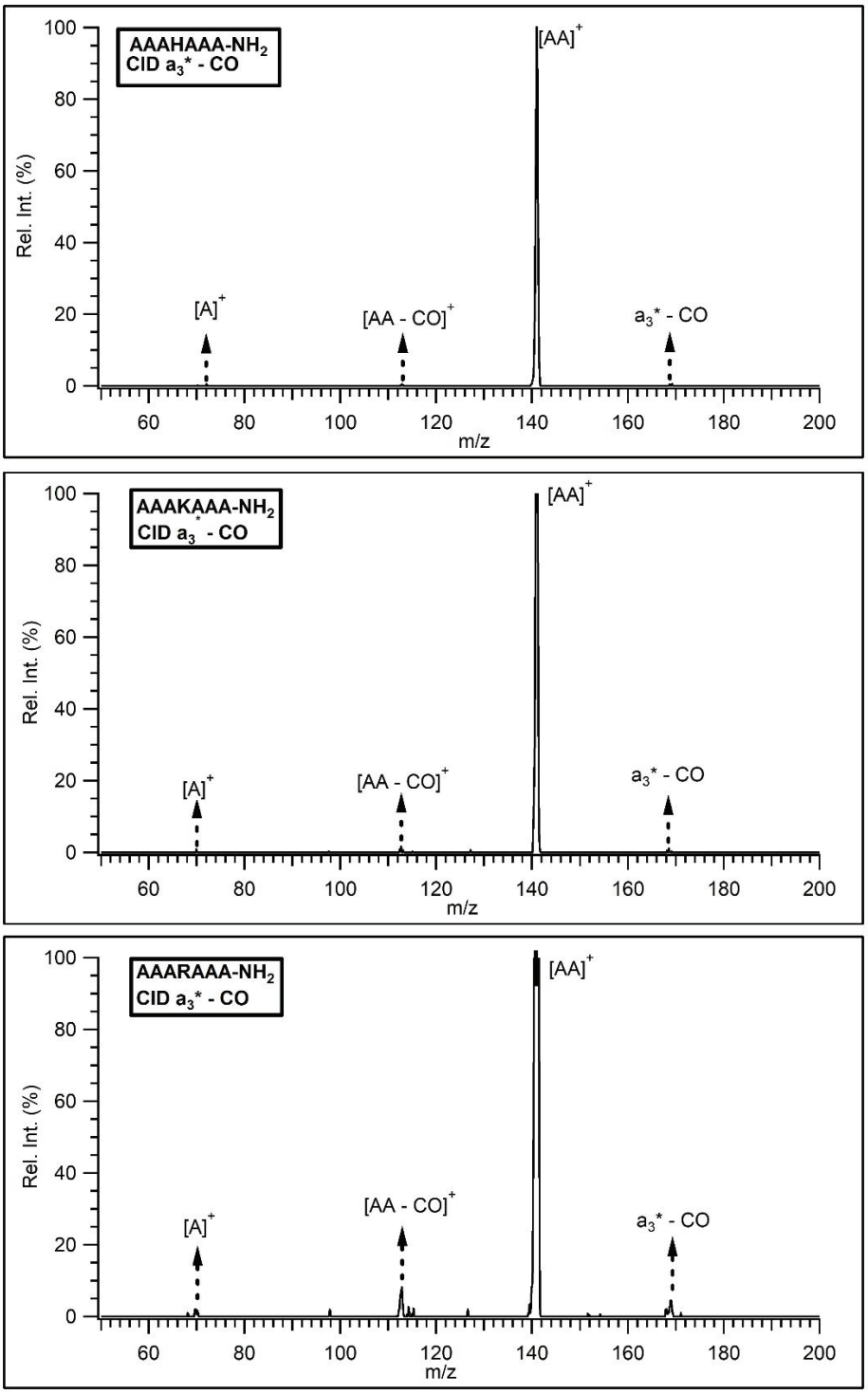

Figure 35. Comparison of a_3^* - CO ion CID mass spectra of AAAHAA-NH_2, AAAKAAA-NH_2 and AAARAAA-NH_2

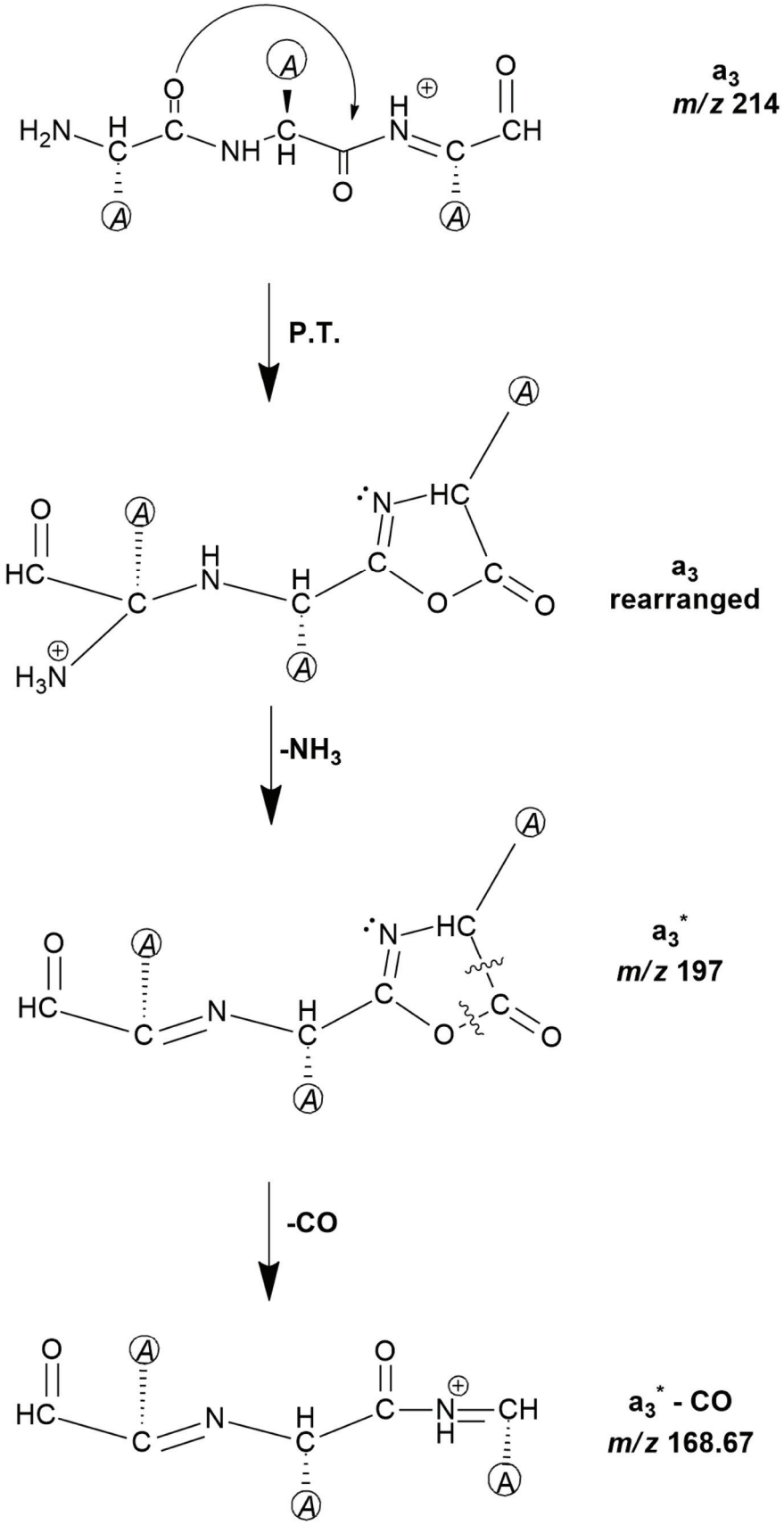

Figure 36. Proposed reaction mechanism for the formation of macrocyclic a_3^* - CO ion in the gas-phase

were observed. Also, some direct sequences such as HYAGFL (b_6^+) (*m/z* 689.0) and HYAGF (b_5^+) (*m/z* 576.0) were found.

Then, His was placed in the middle position and YAGHFLV-NH_2 was performed. Exact same sequences were observed and also a_7^{+2}- Ala (*m/z* 345.0), YAGHFL(b_6^+)-(CO+NH_3) (*m/z* 644.0) and YAGHFL(b_6^+) -59 (*m/z* 630.0). Unfortunately, YAGHFL(b_6^+) -59 (*m/z* 630.0) signal could not be solved.

Finally, YAGFLVH-NH_2 was examined. a_7^{+2} (*m/z* 380.5), a_7^{+2}- NH_3 (*m/z* 372.0), a_7^{+2}- (CO+NH_3) (*m/z* 358.0), a_7^{+2}- (Glycine+NH_3) (*m/z* 343.5), F_{imm} (*m/z* 120.0) and Y_{imm} (*m/z* 136.0) non-direct sequences were obtain.

4.3.2. Lys Residue Containing YAGFLV-NH_2 Peptide Series

Firstly, in Figure 38, doubly-protonated a7 ion CID mass spectrum of KYAGFLV-NH_2, were examined. Fragment ion such as a_7^{+2} (*m/z* 376.0), a_7^{+2}- NH_3 (*m/z* 367.5), a_7^{+2}- (CO+NH_3) (*m/z* 353.58), a_7^{+2}- (Glycine+NH_3) (*m/z* 339.08), KYAGFL (b_6^+) (*m/z* 680.0), KYAGFL (b_6^+)-59 (*m/z* 621.7), KYAGFL (b_6^+) – (glycine+NH_3) (*m/z* 606.0), KYAGF(b_5^+) – CO (*m/z* 539.17), F_{imm} (*m/z* 120.0) and Y_{imm} (*m/z* 136.0) were observed. Moreover, KYAGFL (b_6^+)-59 (*m/z* 621.7) was recorded as an unknown again.

After that, Lys position was changed as a middle again and only a_7^{+2} (*m/z* 376.0), a_7^{+2}- NH_3 (*m/z* 367.5), a_7^{+2}- (CO+NH_3) (*m/z* 353.58), YA(b_2^+) (*m/z* 376.0) and Y_{imm} (*m/z* 136.0) were obtain.

At the final position of Lys, a_7^{+2} (*m/z* 376.0), YAGFLV(b_6^+) (*m/z* 651.0), YAGFLV(b_6^+)-H_2O (*m/z* 633.0), F_{imm} (*m/z* 120.0) and Y_{imm} (*m/z* 136.0) were detected.

4.3.3. Arg Residue Containing YAGFLV-NH_2 Peptide Series

In Figure 39, as a final trial, RYAGFLV-NH_2 was studied. a_7^{+2} (*m/z* 390.0), a_7^{+2}-NH_3 (*m/z* 381.33), a_7^{+2}- (CO+NH_3) (*m/z* 367.67), a_7^{+2}- (Glycine+NH_3) (*m/z* 353.08), RYAGFL(b_6^+) (*m/z* 708.25), RYAGFL(b_6^+) -59 (*m/z* 649.25) F_{imm} (*m/z* 120.0) and Y_{imm} (*m/z* 136.0) were observed.

When the Arg was placed middle position, more fragmentation ions were obtained again such as. a_7^{+2} (*m/z* 390.0), a_7^{+2}- NH_3 (*m/z* 381.33), a_7^{+2}- (CO+NH_3) (*m/z* 367.67), RYAGFL(b_6^+) –(CO+NH_3) (*m/z* 663.0), YAGRFL(b_6^+) (*m/z* 708.17), AGRFLV-NH_2(y_6) -NH_3 (*m/z* 644.0), YAGR (b_4^+) (*m/z* 449.0) and Y_{imm} (*m/z* 136.0).

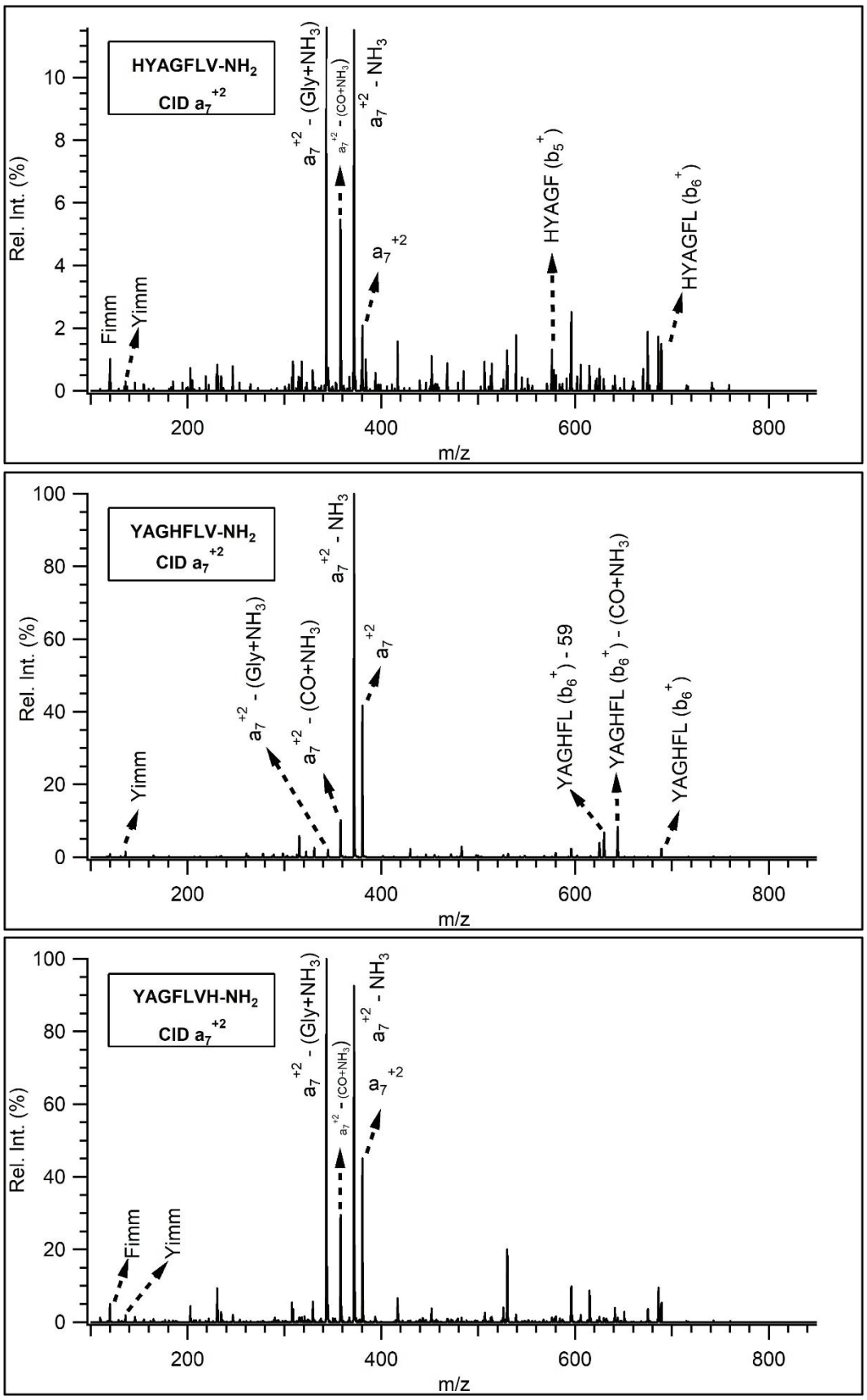

Figure 37. Comparison of a_7^{2+} ion CID mass spectra of HYAGFLV-NH_2, YAGHFLV-NH_2 and YAGFLVH-NH_2

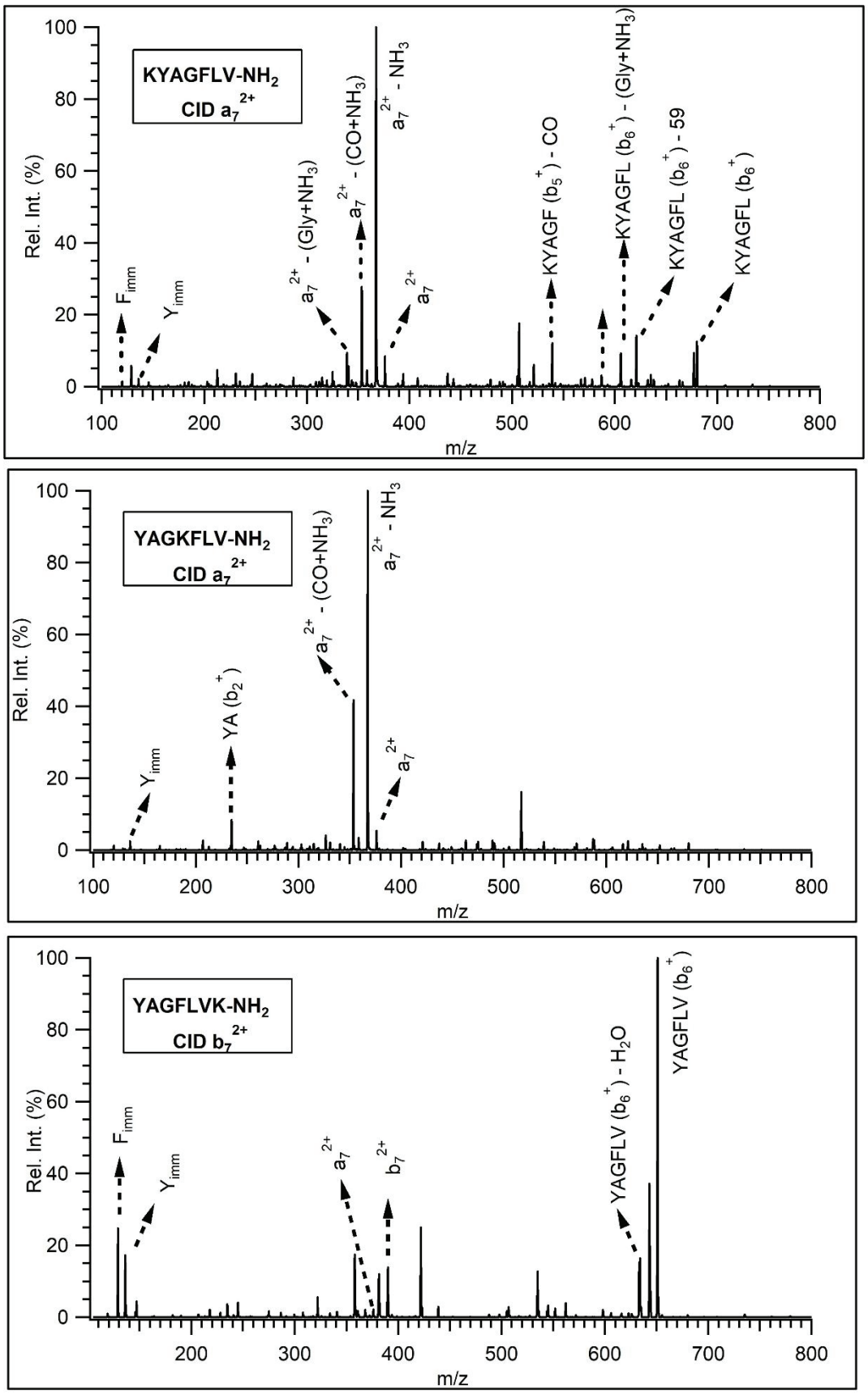

Figure 38. Comparison of a_7^{2+} ion CID mass spectra of KYAGFLV-NH_2, YAGKFLV-NH_2 and YAGFLVK-NH_2

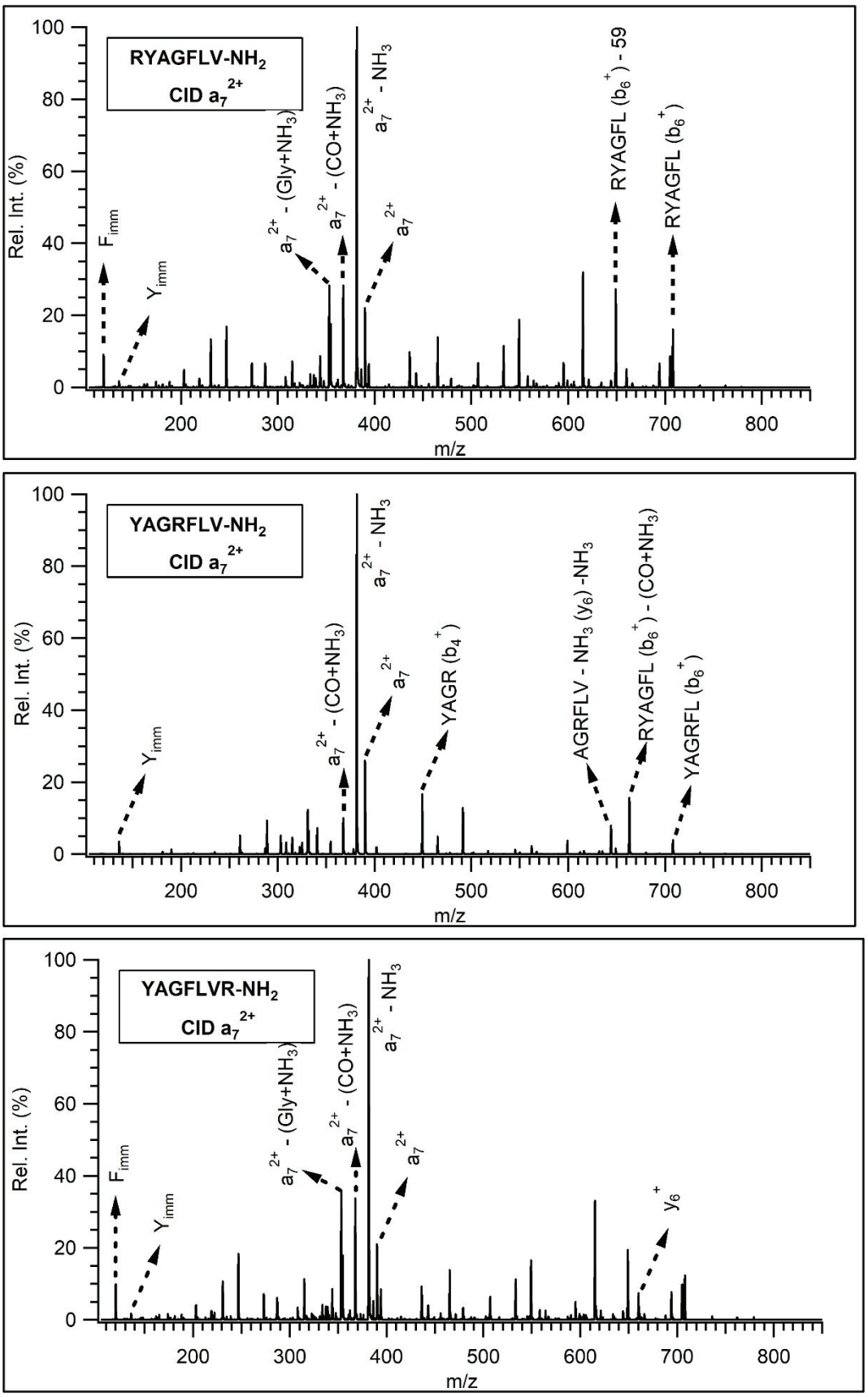

Figure 39. Comparison of a_7^{2+} ion CID mass spectra of RYAGFLV-NH_2, YAGRFLV-NH_2 and YAGFLVR-NH_2

Finally, Arg was placed final position and a_7^{+2} (*m/z* 390.0), a_7^{+2}- NH_3 (*m/z* 381.33), a_7^{+2}- (CO+NH_3) (*m/z* 367.67), a_7^{+2}- (Glycine+NH_3) (*m/z* 353.08), y_6^+ (*m/z* 660.33), F_{imm} (*m/z* 120.0) and Y_{imm} (*m/z* 136.0) were obtained.

4.4. Results and Discussions

Four different doubly-protonated *a* ions were examined using different model peptide series with a variety of amino acid sequencing. The general aspect of the CID spectra of doubly-protonated *a* ions gave similar behavior. Based upon the results three mechanisms were proposed relevant to the macrocyclic behavior of doubly-protonated *a* ions. The interesting result was observed in YAGFLV-NH_2, model peptide series.

Firstly, AAAAAA-NH_2 model peptide series was used because of less reactive features from N-terminal to C-terminal. His, Lys and Arg residues were used for creating doubly-protonated peptides. To investigate position and amino acid effect of His, Lys and Arg residue was located from N-terminal to C-terminal, namely HAAAAAA-NH_2, AHAAAAA-NH_2, AAHAAAA-NH_2, AAAHAAA-NH_2, AAAAHAA-NH_2, AAAAAHA-NH_2, AAAAAAH-NH_2, RAAAAAA-NH_2, ARAAAAA-NH_2, AARAAAA-NH_2, AAARAAA-NH_2, AAAARAA-NH_2, AAAAARA-NH_2, AAAAAAR-NH_2, and KAAAAAA-NH_2, AKAAAAA-NH_2, AAKAAAA-NH_2, AAAKAAA-NH_2, AAAAKAA-NH_2, AAAAAKA-NH_2, AAAAAAK-NH_2, HYAGFLV-NH_2, YAGHFLV-NH_2, YAGFLVH-NH_2, KYAGFLV-NH_2, YAGKFLV-NH_2, YAGFLVK-NH_2, RYAGFLV-NH_2, YAGRFLV-NH_2 and YAGFLVR-NH_2. The CID spectra of a_7^{2+} ions derived from His containing AAAAAA-NH_2 series had the same fragmentations. Moreover, this situation was the same for Lys and Arg containing AAAAAA-NH_2 series. These results can be accepted as a piece of evidence for macrocyclization of *a* ions. According to the proposed mechanism under low CID conditions doubly-protonated peptides loses NH_3 group first and then, doubly-protonated linear oxazolone b_7^{2+} ion is formed. The continuation of this situation is losses of a carbonyl group and so, generation of a_7^{2+} has occurred. After that, amine nitrogen attacks to the adjacent carbon of NH^+ at the C-terminal and "head-to-tail" cyclization takes place. Ring-opening process is completely random and creates the all linear isomers. a_3^* - CO signal was observed in every spectrum.

Secondly, YAGFLV-NH_2 model peptides series were used which including His, Lys and Arg residues from N-termini to C-termini, namely HYAGFLV-NH_2,

YAGHFLV-NH_2, YAGFLVH-NH_2, KYAGFLV-NH_2, YAGKFLV-NH_2, YAGFLVK-NH_2, RYAGFLV-NH_2, YAGRFLV-NH_2, and YAGFLVR-NH_2. The mass spectra of these series were examined under low CID conditions. In general, internal singly-protonated fragments were obtained such as a_7^{+2}, a_7^{+2}- NH_3, a_7^{+2}- (CO+NH_3), a_7^{+2}-(Glycine+NH_3), F_{imm}, Y_{imm}, b_6^+ and some eliminations from the b_6^+ The CID mass spectra of a_7^{+2} ions derived from His, Lys and Arg containing YAGFLV-NH_2 series were quite different and a_7^{2+} signal was too low for all of them. When considering the fragment ions very carefully, there are some similarities among non-direct fragmentation ions, but they are not enough to prove the formation of macrocyclization.

Alanine series were used to compare the position of basic amino acids and proton affinity of basic amino acids among each other, but YAGFLV experiments were helped to understand the formation of macrocyclization among different amino acid residues.

According to the results, type or position of basic amino acid is not affected to generate the a_7^{2+} ion. Macrocyclization can occur every time for Alanine series. However, there was no strong evidence of macrocyclization for YAGFLV series.

CHAPTER 5

CONCLUSION

In this studies, six sets of C-terminal amidated model peptides where the position of basic amino acid residue is varied from N-terminal to C-terminal were used to investigate the macrocyclic behaviour of doubly protonated a_7 ions. It was observed that doubly-protonated a_7 ions produced from these peptides forms a head-to-tail macrocyclization of the corresponding b_7 ions.

This thesis is the first detail study about large doubly charged *a* ions according to our literature knowledge, but lots of new information were observed. Firstly, macrocyclization is occurred for all Alanine series without considering what the basic amino acid is and where the basic amino acid located. Then, a_3^* - CO ion is a common for all Alanine series again. Formation of this fragmentation was also studied and proposed a mechanism for that. Results were proved that, the formation of a_3^* - CO fragment includes only Alanine amino acid and further fragmentations. Furthermore, water elimination (- H_2O) was observed for all Alanine series.

In YAGFLV series, a_7^{+2}, a_7^{+2} - NH_3 elimination and a_7^{+2} - (CO+NH_3) elimination are observed all YAGFLV series except YAGFLVK. Besides, a_7^{+2}- (Glycine+NH_3) elimination is also observed for the all YAGFLV series except YAGRFLV, YAGFLVK, and YAGKFLV. According to these results, there was no strong evidence of macrocyclization for YAGFLV series. The peptides which have YAGFLV series might be more stable as a linear than the macrocycle structure. Therefore, different length of *a* ions should be studied in both Alanine and YAGFLV series and the other amino acids should be studied instead of the basic ones to see doubly charged *a* ions.

REFERENCES

1. Wang, Y.; Sun, J.; Qiao, J.; Ouyang, J.; Na, N., A "Soft" and "Hard" Ionization Method for Comprehensive Studies of Molecules. *Analytical Chemistry* **2018,** *90* (24), 14095-14099.

2. Banerjee, S.; Mazumdar, S., Electrospray ionization mass spectrometry: a technique to access the information beyond the molecular weight of the analyte. *Int J Anal Chem* **2012,** *2012*, 282574.

3. Wilm, M., Principles of electrospray ionization. *Mol Cell Proteomics* **2011,** *10* (7), M111 009407.

4. Murphy, R. C.; Barkley, R. M.; Zemski Berry, K.; Hankin, J.; Harrison, K.; Johnson, C.; Krank, J.; McAnoy, A.; Uhlson, C.; Zarini, S., Electrospray ionization and tandem mass spectrometry of eicosanoids. *Analytical Biochemistry* **2005,** *346* (1), 1-42.

5. Yalcin, E. B.; de la Monte, S. M., Review of matrix-assisted laser desorption ionization-imaging mass spectrometry for lipid biochemical histopathology. *J Histochem Cytochem* **2015,** *63* (10), 762-71.

6. Dreisewerd, K., The Desorption Process in MALDI. *Chemical Reviews* **2003,** *103* (2), 395-426.

7. Zenobi, R.; Knochenmuss, R., *Ion formation in MALDI mass spectrometry*. 1998; Vol. 17.

8. Knochenmuss, R.; Zenobi, R., MALDI Ionization: The Role of In-Plume Processes. *Chemical Reviews* **2003,** *103* (2), 441-452.

9. Tholey, A.; Heinzle, E., Ionic (liquid) matrices for matrix-assisted laser desorption/ionization mass spectrometry-applications and perspectives. *Anal Bioanal Chem* **2006,** *386* (1), 24-37.

10. Suckau, D.; Resemann, A.; Schuerenberg, M.; Hufnagel, P.; Franzen, J.; Holle, A., A novel MALDI LIFT-TOF/TOF mass spectrometer for proteomics. *Anal Bioanal Chem* **2003,** *376* (7), 952-65.

11. El-Aneed, A.; Cohen, A.; Banoub, J., Mass Spectrometry, Review of the Basics: Electrospray, MALDI, and Commonly Used Mass Analyzers. *Applied Spectroscopy Reviews* **2009,** *44* (3), 210-230.

12. Glish, G. L.; Vachet, R. W., The basics of mass spectrometry in the twenty-first century. *Nat Rev Drug Discov* **2003,** *2* (2), 140-50.

13. March, R. E., Quadrupole ion traps. *Mass Spectrom Rev* **2009,** *28* (6), 961-89.

14. Douglas, D. J.; Konenkov, N. V., Trajectory calculations of space-charge-induced mass shifts in a linear quadrupole ion trap. *Rapid Commun Mass Spectrom* **2012,** *26* (18), 2105-14.

15. Dehmelt, H. G., Radiofrequency Spectroscopy of Stored Ions I: Storage. In *Advances in Atomic and Molecular Physics Volume 3*, 1968; pp 53-72.

16. Nolting, D.; Malek, R.; Makarov, A., Ion traps in modern mass spectrometry. *Mass Spectrom Rev* **2019,** *38* (2), 150-168.

17. Hoffman, E.; Stroobant, V., Mass Spectrometry Principles and Applicaitons. 3 ed. *John Wiley & Sons:* **2007,** *England*.

18. B. A. Mamyrin; V. I. Karataev; D. V. Shmikk; Zagulin, V. A., The mass-reflectron, a new nonmagnetic time-of-flight mass spectrometer with high resolution. *Zh. Eksp. Teor. Fiz,* **1972,** *64* (82-89).

19. Scigelova, M.; Hornshaw, M.; Giannakopulos, A.; Makarov, A., Fourier transform mass spectrometry. *Mol Cell Proteomics* **2011,** *10* (7), M111 009431.

20. Makarov, A., Electrostatic Axially Harmonic Orbital Trapping: A High-Performance Technique of Mass Analysis. *HD Technologies Ltd., Atlas House, Simonsway, Manchester, M22 5PP, U.K.* **2000,** *72* (1156-1162).

21. Neetu, K.; Ankit, G.; Ruchi, T.; Ajay, B.; Prashant, B., A Review on Mass Spectrometry Detectors. *International Research Journal of Pharmacy* **2012,** *3* (10), 33-42.

22. Ladislas Wiza, J., Microchannel plate detectors. *Nuclear Instruments and Methods 162* (1-3), 587-601.

23. Dass, C., Principles and Practice of Biological Mass Spectrometry. *Wiley Interscience: New York* **2001**.

24. Wysocki, V. H.; Tsaprailis, G.; Smith, L. L.; Breci, L. A., Special feature: Commentary - Mobile and localized protons: a framework for understanding peptide dissociation. *Journal of Mass Spectrometry* **2000,** *35* (12), 1399-1406.

25. Dongré, A. R.; Jones, J. L.; Somogyi, Á.; Wysocki, V. H., Influence of Peptide Composition, Gas-Phase Basicity, and Chemical Modification on Fragmentation Efficiency: Evidence for the Mobile Proton Model. *Journal of the American Chemical Society* **1996,** *118* (35), 8365-8374.

26. Rodriquez, C. F.; Cunje, A.; Shoeib, T.; Chu, I. K.; Hopkinson, A. C.; Siu, K. W. M., Proton Migration and Tautomerism in Protonated Triglycine. *Journal of the American Chemical Society* **2001,** *123* (13), 3006-3012.

27. Paizs, B.; Suhai, S., Fragmentation pathways of protonated peptides. *Mass Spectrom Rev* **2005,** *24* (4), 508-48.

28. Hughes, C.; Ma, B.; Lajoie, G. A., De novo sequencing methods in proteomics. *Methods Mol Biol* **2010,** *604*, 105-21.

29. Black, D. L., Protein Diversity from Alternative Splicing: A Challenge for Bioinformatic and Post-Genome Biology. *Cell* **2000,** *103*, 367-370.

30. Cooper, H. J.; Hakansson, K.; Marshall, A. G., The role of electron capture dissociation in biomolecular analysis. *Mass Spectrom Rev* **2005,** *24* (2), 201-22.

31. Paizs, B.; Lendvay, G.; Vékey, K.; Suhai, S., Formation of b2+ ions from protonated peptides: an ab initio study. *Rapid Communications in Mass Spectrometry* **1999** *13* (6), 525-533.

32. Polce, M. J.; Ren, D.; Wesdemiotis, C., Dissociation of the peptide bond in protonated peptides. *Journal of Mass Spectrometry* **2000,** *35* (12), 1391-1398.

33. Yalcin, T.; Csizmadia, I. G.; Peterson, M. R.; Harrison, A. G., The structure and fragmentation of Bn(n≥3) ions in peptide spectra. *Journal of the American Society for Mass Spectrometry* **1996,** *7* (3), 233-242.

34. Yalcin, T.; Khouw, C.; Csizmadia, I. G.; Peterson, M. R.; Harrison, A. G., Why Are B ions stable species in peptide spectra? *Journal of the American Society for Mass Spectrometry* **1995,** *6* (12), 1165-1174.

35. Tang, X. J.; Boyd, R. K., An Investigation of Fragmentation Mechanisms of Doubly Protonated Tryptic Peptides. *Rapid Communications in Mass Spectrometry* **1992,** *6* (11), 651-657.

36. Harrison, A. G., Charge-separation reactions of doubly-protonated peptides: Effect of peptide chain length. *Journal of the American Society for Mass Spectrometry* **2009,** *20* (10), 1890-1895.

37. Knapp-Mohammady, M.; Young, A. B.; Paizs, B.; Harrison, A. G., Fragmentation of doubly-protonated Pro-His-Xaa tripeptides: Formation of b22+ions. *Journal of the American Society for Mass Spectrometry* **2009,** *20* (11), 2135-2143.

38. Grewal, R. N.; El Aribi, H.; Harrison, A. G.; Siu, K. W. M.; Hopkinson, A. C., Fragmentation of Protonated Tripeptides: The Proline Effect Revisited. *The Journal of Physical Chemistry B* **2004,** *108* (15), 4899-4908.

39. Shi, T.; Siu, K. W. M.; Hopkinson, A. C., Generation of [La(peptide)]3+ Complexes in the Gas Phase: Determination of the Number of Binding Sites Provided by Dipeptide, Tripeptide, and Tetrapeptide Ligands. *The Journal of Physical Chemistry A* **2007,** *111* (45), 11562-11571.

40. Tabb, D. L.; Huang, Y.; Wysocki, V. H.; Yates, J. R., Influence of Basic Residue Content on Fragment Ion Peak Intensities in Low-Energy Collision-Induced Dissociation Spectra of Peptides. *Analytical Chemistry* **2004,** *76* (5), 1243-1248.